

The concept of quasi-integrability: a concrete example

L. A. Ferreira ^{*}, and Wojtek J. Zakrzewski [†]

(^{*})Instituto de Física de São Carlos; IFSC/USP;
Universidade de São Paulo
Caixa Postal 369, CEP 13560-970, São Carlos-SP, Brazil

([†]) Department of Mathematical Sciences,
University of Durham, Durham DH1 3LE, U.K.

Abstract

We use the deformed sine-Gordon models recently presented by Bazeia et al [1] to discuss possible definitions of quasi-integrability. We present one such definition and use it to calculate an infinite number of quasi-conserved quantities through a modification of the usual techniques of integrable field theories. Performing an expansion around the sine-Gordon theory we are able to evaluate the charges and the anomalies of their conservation laws in a perturbative power series in a small parameter which describes the “closeness” to the integrable sine-Gordon model. Our results indicate that in the case of the two-soliton scattering the charges are conserved asymptotically, *i.e.* their values are the same in the distant past and future, when the solitons are well separated.

We back up our results with numerical simulations which also demonstrate the existence of long lived breather-like and wobble-like states in these models.

1 Introduction

Solitons and integrable field theories play a central role in the study of many non-linear phenomena. Indeed, it is perhaps correct to say that many non-perturbative and exact methods known in field theories are in one way or the other related to solitons. The reason for that is twofold. On one hand, the appearance of solitons in a given theory is often related to a high degree of symmetries and so to the existence of a large number of conservation laws. On the other hand, in a large class of theories the solitons possess a striking property. They become weakly coupled when the interaction among the fundamental particles of the theory is strong, and vice-versa. Therefore, the solitons are the natural candidates to describe the relevant normal modes in the strong coupling (non-perturbative) regime of the theory. Such relation between the strong and weak coupling regimes have been observed in some (1+1) dimensional field theories, as, for example, in the equivalence of the sine-Gordon and Thirring models [2], as well as in four dimensional supersymmetric gauge theories where monopoles (solitons) and fundamentals gauge particles exchange roles in the so-called duality transformations [3].

The exact methods to study solitons in (1 + 1)-dimensional field theories involve many algebraic and geometrical concepts, but the most important ingredient is the so-called zero curvature condition or the Lax-Zakharov-Shabat equation [4]. All theories known to possess exact soliton solutions admit a representation of their equations of motion as a zero curvature condition for a connection living in an infinite dimensional Lie (Kac-Moody) algebra [5, 6]. In fact, in (1 + 1) dimensions such zero curvature condition is a conservation law, and the conserved quantities are given by the eigenvalues of the holonomy of the flat connection calculated on a spatial (fixed time) curve. On the other hand, many techniques, like the dressing transformation method, for the construction of exact solutions are based on the zero curvature condition. In dimensions higher than two the soliton theory is not so well developed, even though many exact results are known for some 2-dimensional theories such as the CP^N models [7], as well as in four dimensional gauge theories where instanton and self-dual monopoles are the best examples [8]. Some approaches have been proposed for the study of integrable field theories in higher dimensions based on generalizations of the two dimensional methods like the tetrahedron equations [9] and of the concept of zero curvature involving connections in loop spaces [10].

Another important aspect of integrable field theories is that they serve as good approximations to many physical phenomena. In fact, there is a vast literature exploring many aspects and applications of perturbations around integrable models. In this paper we want to put forward a technique that, so far as we know, has not been explored yet and which suggests that some non-integrable theories often possess many important properties of fully integrable ones. We put forward and develop the concept of quasi-integrability for theories

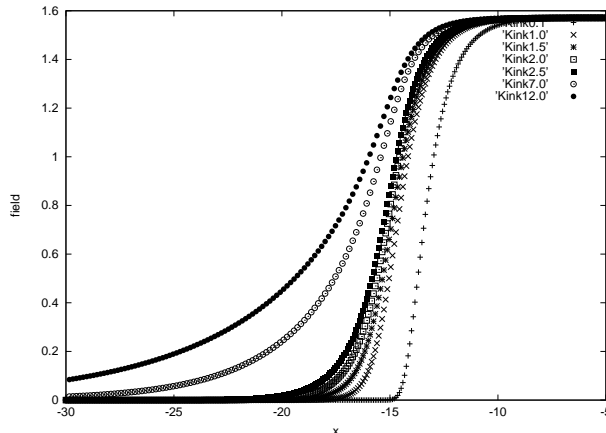


Figure 1: Plots of solitons for various values on n

that do not admit a representation of their equations of motion in terms of the Lax-Zakharov-Shabat equation, but which can, nevertheless, be associated with an almost flat connection in an infinite dimensional Lie algebra. In other words, we have an anomalous zero curvature condition that leads to an infinite number of quasi-conservation (almost conservation) laws.

Moreover, in practice, in physical situations, like the scattering of solitons, these charges are effectively conserved. The striking property we have discovered is that as the scattering process takes place the charges do vary in time. However, after the solitons have separated from each other the charges return to the values they had prior to the scattering. Effectively what we have is the asymptotic conservation of an infinite number of non-trivial charges. There are still several aspects of this observation that have to be better understood but we believe that if our results are indeed robust then such asymptotic charges could play a role in many important properties of the theory like the factorization of the S-matrix.

We introduce our concept of quasi-integrability through a concrete example involving a real scalar field theory in $(1+1)$ dimensions which is a special deformation of the sine-Gordon model. The scalar field φ of our theory is subjected to the potential

$$V(\varphi, n) = \frac{2}{n^2} \tan^2 \varphi [1 - |\sin \varphi|^n]^2 \quad (1.1)$$

where n is a real parameter which in the case $n = 2$ reduces the potential to that of the sine-Gordon model, *i.e.* $V(\varphi, 2) = \frac{1}{16} [1 - \cos(4\varphi)]$.

This potential (1.1) is a slight modification of that introduced by D. Bazeia et al, [1], in the sense that we take the absolute value of $\sin \varphi$ to allow n to take real and not only integer values.

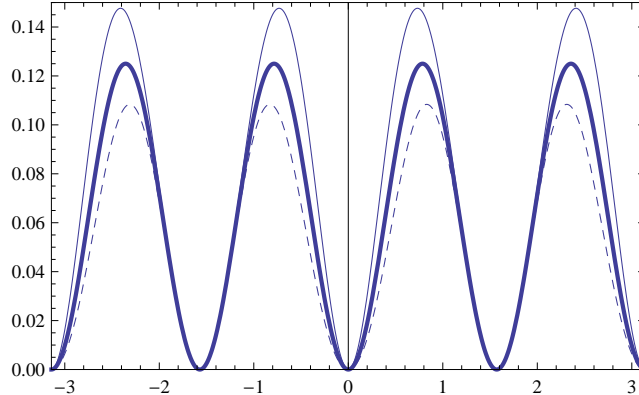


Figure 2: Plots of the potential (1.1) against φ , for three values of the parameter ε , where $n = 2 + \varepsilon$, namely $\varepsilon = -0.5$ (fine line), $\varepsilon = 0.0$ (thick line), and $\varepsilon = 0.5$ (dashed line).

The potential (1.1) has an infinite number of degenerate vacua that allow the existence of solutions with non-trivial topological charges. It is worth noticing that the positions of the vacua are independent of n and so they are the same as in the sine-Gordon model, *i.e.* $\varphi_{\text{vac.}} = m \frac{\pi}{2}$, with m being any integer.

The model with the potential (1.1) is fully topological (*i.e.* it satisfies its Bogomolnyi bound for any n) and so its one soliton field configurations are known in an explicit form. They are given by:

$$\varphi = \arcsin \left[\frac{e^{2\Gamma}}{1 + e^{2\Gamma}} \right]^{1/n}, \quad \Gamma = \pm \frac{(x - vt - x_0)}{\sqrt{1 - v^2}}, \quad (1.2)$$

where the velocity v is given in units of the speed of light, and the signs correspond to the kink (+), and anti-kink (-), with topological charges +1, and -1 respectively. In Figure 1 we plot the fields of a one soliton configuration for various values on n . We see from this plot that the $n = 2$ case does not appear to be very special; all soliton fields look very similar and the solitons for different values of n differ only in their slopes.

We are going to use this model to back up our discussion of quasi-integrability and so next we look at $n = 2 + \varepsilon$, with ε small. In Figure 2 we plot the potential (1.1) for $\varepsilon = -0.5; 0.0; 0.5$. Of course, in this case the kinks solutions are given by (1.2) with n replaced by $2 + \varepsilon$. In Figure 3 we plot the one kink solutions (1.2) for the potentials shown in Figure 2, *i.e.* for $\varepsilon = -0.5; 0.0; 0.5$. Note that they connect the vacua $\varphi_{\text{vac}} = 0$ to $\varphi_{\text{vac.}} = \frac{\pi}{2}$, as x goes from $-\infty$ to $+\infty$, with the slope of the kink increasing as the value of ε decreases.

In this paper we study the concept of quasi-integrability in the context of the theory (1.1)

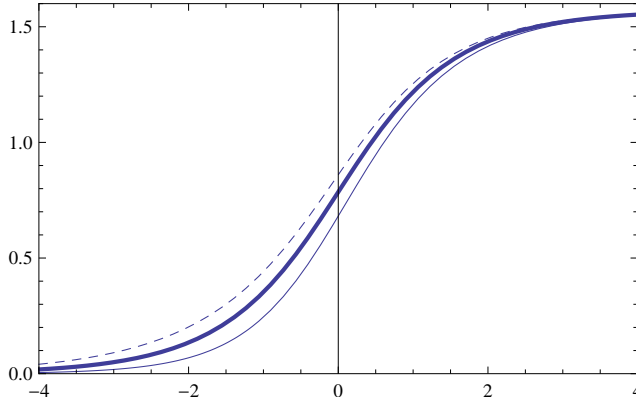


Figure 3: Plots of the kink solutions (1.2) against x , with $t = 0$ and $x_0 = 0$, for three values of the parameter ε , where $n = 2 + \varepsilon$, namely $\varepsilon = -0.5$ (fine line), $\varepsilon = 0.0$ (thick line), and $\varepsilon = 0.5$ (dashed line).

from the analytical and numerical points of view¹. Our approach and the main results of this paper can be summarised as follows (more details are given in the following sections):

We first consider a real scalar field theory with a very general potential $V(\varphi)$, and construct a connection A_μ based on the $sl(2)$ loop algebra which, as a consequence of its equations of motion, satisfies an anomalous zero curvature condition. Using a modification of the methods employed in integrable field theories we construct an infinite number of quasi-conserved charges for such a theory, *i.e.*

$$\frac{dQ^{(2n+1)}}{dt} = -\frac{1}{2}\alpha^{(2n+1)}(t) \quad n = 0, \pm 1, \pm 2, \dots, \quad (1.3)$$

where the anomalies $\alpha^{(2n+1)}(t)$ are non-zero due to the non-flatness of the connection A_μ . The charges $Q^{(\pm 1)}$ are in fact conserved, *i.e.* $\alpha^{(\pm 1)} = 0$, and linear combinations of them correspond to the energy and momentum.

We then restrict ourselves to the case of the potential (1.1) and set up a perturbative expansion around the sine-Gordon theory. We expand all the quantities, equations of motion, field φ , charges and anomalies, in powers of the parameter ε , related to n appearing in (1.1) by $n = 2 + \varepsilon$. For instance, we have

$$Q^{(2n+1)} = Q_0^{(2n+1)} + \varepsilon Q_1^{(2n+1)} + O(\varepsilon^2), \quad \alpha^{(2n+1)} = \varepsilon \alpha_1^{(2n+1)} + O(\varepsilon^2). \quad (1.4)$$

The anomalies vanish in the lowest order (order zero) in ε because they correspond to the

¹Preliminary results of our approach have already been given in [11]

sine-Gordon theory which is integrable and so all the charges $Q_0^{(2n+1)}$ are conserved during the dynamics of all field configurations.

In this paper we concentrate our attention on the evaluation of the first non-trivial charge and its anomaly, namely $Q^{(3)}$ and $\alpha^{(3)}$, but our calculations can easily be extended to the other charges. We considered the case of the scattering of two kinks and also of a kink/anti-kink in the theory (1.1), where the solitons are far apart in the distant past and future, and collide when $t \sim 0$. We found that the first order anomaly $\alpha_1^{(3)}$, vanishes when integrated over the whole time axis. Therefore, from (1.3) we see that

$$Q_1^{(3)}(t = +\infty) = Q_1^{(3)}(t = -\infty). \quad (1.5)$$

Consequently, the scattering of the solitons happen in a way that, to first order in ε at least, the charge is asymptotically conserved. That is a very important result, and if one can extend it to higher orders and higher charges one would prove that effectively the scattering of solitons in the theory (1.1) takes place in the same way as if the theory were a truly integrable theory. We have also analyzed the first order charge $Q_1^{(3)}$ for the breather solution of the theory (1.1), and found that even though the charge is not conserved, it oscillates around a fixed value. In other words, the first order anomaly vanishes when integrated over a period $\frac{\pi}{\nu}$, and so from (1.3) we find that

$$Q_1^{(3)}(t) = Q_1^{(3)}\left(t + \frac{\pi}{\nu}\right), \quad (1.6)$$

where ν is the angular frequency of the breather. That means that the period of the charge is half of that of the breather.

We have performed many numerical simulations of the full theory (1.1) using a fourth order Runge-Kuta method, and using various lattice grids to make sure that the results are not contaminated by numerical artifacts. We have found reliable results with lattice grids of at least 3001 points, where the kinks were of size ~ 5 points. Most of the simulations in this paper were performed with lattices of 10001 points (*i.e.* well within this reliability). The main results we have found are the following: We have found that if $|\varepsilon|$ does not get very close to unity the kinks and the kink/anti-kink scatter without destroying themselves and preserve their original shapes, given in (1.2). For small values of $|\varepsilon|$ the anomaly $\alpha^{(3)}$ integrates to zero for large values of the time interval, and so the charge $Q^{(3)}$ is asymptotically conserved within our numerical errors. This is an important confirmation of our analytical result described above, and is valid for the full charge and not only for its first order approximation as in (1.5).

One of the important discoveries of our numerical simulations is that the theory (1.1) also possesses very long lived breather solutions for $\varepsilon \neq 0$, which correspond to non-integrable models. These long-lived breathers were obtained by starting the simulations with a field configuration corresponding to a kink and an anti-kink. As they get close to each other

they interact and readjust their profiles and some radiation is emitted in this process. We absorbed this radiation at the boundaries of the grid and the system stabilized to a breather-like configuration. For $n = 2$ the resultant field configuration was the exact (and analytically known) breather while for ε small those breather-like fields lived for millions of units of time. As one changed ε and made it come close to unity the quasi-breathers radiated more and for even larger values they eventually died. We also looked at the anomalies for such breather-like configurations and have found a good agreement with our analytical results described above. The anomaly, integrated in time, does oscillate and for small values of ε the charge is periodic in time. That is, again, in agreement with the analytical result (1.6). Notice however, that the numerical result is stronger in the sense that it corresponds to the full charge and not only to its first order approximation as in (1.6).

We have also performed similar numerical simulations of wobbles [12] which correspond to configurations of a breather and a kink. Again, such configurations were obtained by starting the simulation with two kinks and an anti-kink. As the three solitons interact and adjust their profiles they radiate energy and this radiation had been absorbed at the boundaries of the grid. Eventually the system has evolved to a breather and a kink and for small values of ε the resultant configuration was quite stable, and for $n = 2$ it agreed with the analytically known configuration of a wobble. Again, we believe that this is a very interesting result which shows that non-integrable theories can support such kinds of solutions.

Our results open up the way to investigate large classes of models which are not really exactly integrable but which possess properties which are very similar to those of integrable field theories. We believe that they will have applications in many non-linear phenomena of physical interest.

The paper is organized as follow: in section 2 we introduce the quasi-zero curvature condition, based on the $sl(2)$ loop algebra, for a real scalar field theory subject to a generic potential, and construct an infinite number of quasi-conserved quantities. In section 3 we perform the expansion of the theory (1.1) around the sine-Gordon model, and evaluate the first non-trivial charge and its corresponding anomaly. The numerical simulations, involving the two solitons scattering, breathers and a wobble, are presented in section 4. In section 5 we present our conclusions; the details of the $sl(2)$ loop algebra, charge calculations and ε -expansion are presented in the appendices.

2 The quasi zero curvature condition

We shall consider Lorentz invariant field theories in $(1+1)$ -dimensions with a real scalar field φ and equation of motion given by

$$\partial^2 \varphi + \frac{\partial V(\varphi)}{\partial \varphi} = 0, \quad (2.1)$$

where $V(\varphi)$ is the scalar potential. Thus we want to study the integrability properties of such theory using the techniques of integrable field theories [4, 5, 6]. We then start by trying to set up a zero curvature representation of the equations of motion (2.1), and so we introduce the Lax potentials as

$$\begin{aligned} A_+ &= \frac{1}{2} \left[(\omega^2 V - m) b_1 - i\omega \frac{dV}{d\varphi} F_1 \right], \\ A_- &= \frac{1}{2} b_{-1} - \frac{i}{2} \omega \partial_- \varphi F_0. \end{aligned} \quad (2.2)$$

Our Lax potentials live on the so-called $sl(2)$ loop algebra with generators b_{2n+1} and F_n , with n integer; their commutation relations are given in Appendix A. The parameters ω and m are constants, and they play a special role in our analysis. Note, that the dynamics governed by (2.1) does not depend upon them, but since they appear in (2.2) they will play a role in the quasi-conserved quantities that we will construct through the Lax equations. In the expression above we have used light cone coordinates $x_{\pm} = \frac{1}{2}(t \pm x)$, where $\partial_{\pm} = \partial_t \pm \partial_x$, and $\partial_+ \partial_- = \partial_t^2 - \partial_x^2 \equiv \partial^2$.

The curvature of the connection (2.2) is given by

$$F_{+-} \equiv \partial_+ A_- - \partial_- A_+ + [A_+, A_-] = X F_1 - \frac{i\omega}{2} \left[\partial^2 \varphi + \frac{\partial V}{\partial \varphi} \right] F_0 \quad (2.3)$$

with

$$X = \frac{i\omega}{2} \partial_- \varphi \left[\frac{d^2 V}{d\varphi^2} + \omega^2 V - m \right]. \quad (2.4)$$

As in the case of the sine-Gordon model where the potential is given by

$$V_{\text{SG}} = \frac{1}{16} [1 - \cos(4\varphi)] \quad (2.5)$$

we find that X , given by (2.4), vanishes when we take $\omega = 4$ and $m = 1$. Then the curvature (2.3) vanishes when the equations of motion (2.1) hold. The vanishing of the curvature allows us to use several powerful techniques to construct conserved charges and exact solutions. We want to analyze what can be said about the conservation laws for potentials when X does not vanish but can be considered small.

In general, the conserved charges can be constructed using the fact that the path ordered integral of the connection along a curve Γ , namely $P \exp \left[\int_{\Gamma} d\sigma A_{\mu} \frac{dx^{\mu}}{d\sigma} \right]$, is path independent when the connection is flat [5, 6, 13]. Here, we will use a more refined version of this technique and try to gauge transform the connection into the abelian subalgebra generated by the b_{2n+1} . We follow the usual procedures of integrable field theories discussed for instance in [14, 15, 16]. An important ingredient of the method is that our $sl(2)$ loop algebra \mathcal{G} is graded, with n being the grades determined by the grading operator $d = T_3 + 2\lambda \frac{d}{d\lambda}$ (see appendix A for details)

$$\mathcal{G} = \sum_n \mathcal{G}_n ; \quad [\mathcal{G}_m, \mathcal{G}_n] \subset \mathcal{G}_{m+n} ; \quad [d, \mathcal{G}_n] = n \mathcal{G}_n. \quad (2.6)$$

We perform a gauge transformation

$$A_{\mu} \rightarrow a_{\mu} = g A_{\mu} g^{-1} - \partial_{\mu} g g^{-1} \quad (2.7)$$

with the group element g being an exponentiation of generators lying in the positive grade subspace generated by the F_n 's, *i.e.*,

$$g = \exp \left[\sum_{n=1}^{\infty} \zeta_n F_n \right] \quad (2.8)$$

with ζ_n being parameters to be determined as we will explain below. Under (2.7) the curvature (2.3) is transformed as

$$F_{+-} \rightarrow g F_{+-} g^{-1} = \partial_+ a_- - \partial_- a_+ + [a_+, a_-] = X g F_1 g^{-1}, \quad (2.9)$$

where we have used the equations of motion (2.1) to drop the term proportional to F_0 in (2.3). The component A_- of the connection (2.2) has terms with grade 0 and -1 . Therefore, under (2.7) it is transformed into a_- which has terms with grades ranging from -1 to $+\infty$. Decomposing a_- into grades we get from (2.7) and (2.8) that

$$\begin{aligned} a_- &= \frac{1}{2} b_{-1} \\ &- \frac{1}{2} \zeta_1 [b_{-1}, F_1] - \frac{i}{2} \omega \partial_- \varphi F_0 \\ &- \frac{1}{2} \zeta_2 [b_{-1}, F_2] + \frac{1}{4} \zeta_1^2 [[b_{-1}, F_1], F_1] - \frac{i}{2} \omega \partial_- \varphi \zeta_1 [F_1, F_0] - \partial_- \zeta_1 F_1 \\ &\vdots \\ &- \frac{1}{2} \zeta_n [b_{-1}, F_n] + \dots \end{aligned} \quad (2.10)$$

Next we note that one can choose the parameters ζ_n recursively by requiring that the component in the direction on F_{n-1} cancels out in a_- . Thus we can put that $\zeta_1 = \frac{i}{2} \omega \partial_- \varphi$,

and so on. In the appendix B we give the first few ζ_n 's obtained that way. In consequence, the component a_- is rotated into the abelian subalgebra generated by the b_{2n+1} . Note that this procedure has not used the equations of motion (2.1). We then have

$$a_- = \frac{1}{2} b_{-1} + \sum_{n=0}^{\infty} a_-^{(2n+1)} b_{2n+1} \quad (2.11)$$

and the first three components are

$$\begin{aligned} a_-^{(1)} &= -\frac{1}{4} \omega^2 (\partial_- \varphi)^2, \\ a_-^{(3)} &= -\frac{1}{16} \omega^4 (\partial_- \varphi)^4 - \frac{1}{4} \omega^2 \partial_-^3 \varphi \partial_- \varphi, \\ a_-^{(5)} &= -\frac{1}{32} \omega^6 (\partial_- \varphi)^6 - \frac{7}{16} \omega^4 \partial_-^3 \varphi (\partial_- \varphi)^3 - \frac{11}{16} \omega^4 (\partial_-^2 \varphi)^2 (\partial_- \varphi)^2 - \frac{1}{4} \omega^2 \partial_-^5 \varphi \partial_- \varphi. \end{aligned} \quad (2.12)$$

With the ζ_n 's determined this way we perform the transformation of the A_+ component of the connection (2.2). Since the ζ_n 's are polynomials of x_- -derivatives of φ (see appendix B) and since there will be terms involving x_+ -derivatives of ζ_n 's, we use the equations of motion to eliminate terms involving $\partial_+ \partial_- \varphi$. Due to the nonvanishing of the anomaly term X in (2.3) we are not able to transform a_+ into the abelian subalgebra generated by the b_{2n+1} . We find that a_+ is of the form

$$a_+ = \sum_{n=0}^{\infty} a_+^{(2n+1)} b_{2n+1} + \sum_{n=2}^{\infty} c_+^{(n)} F_n \quad (2.13)$$

where

$$\begin{aligned} a_+^{(1)} &= \frac{1}{2} [\omega^2 V - m], \\ a_+^{(3)} &= \frac{1}{4} \omega^2 \partial_-^2 \varphi \frac{dV}{d\varphi} - \frac{1}{2} i \omega \partial_- \varphi X, \\ a_+^{(5)} &= -\frac{3}{8} i \omega^3 (\partial_- \varphi)^3 X + \frac{5}{16} \omega^4 \partial_-^2 \varphi (\partial_- \varphi)^2 \frac{dV}{d\varphi} - \frac{1}{2} i \omega \partial_- \varphi \partial_-^2 X + \frac{1}{2} i \omega \partial_-^2 \varphi \partial_- X \\ &\quad - \frac{1}{2} i \omega \partial_-^3 \varphi X + \frac{1}{4} \omega^2 \partial_-^4 \varphi \frac{dV}{d\varphi} \end{aligned} \quad (2.14)$$

with X given in (2.4), and V being the potential (see (2.1)). See appendix B for more details, including the terms involving $c_+^{(n)}$.

The next step is to decompose the curvature (2.9) into the component lying in the abelian subalgebra generated by b_{2n+1} and one lying in the subspace generated by F_n . Since the equation of motion (2.1) has been imposed, it turns out that the terms proportional to the F_n 's in the combination $-\partial_- a_+ + [a_+, a_-] - X g F_1 g^{-1}$, exactly cancel out. We are then left

with terms in the direction of the b_{2n+1} only. Therefore, the transformed curvature (2.9) leads to equations of the form

$$\partial_+ a_-^{(2n+1)} - \partial_- a_+^{(2n+1)} = \beta^{(2n+1)} \quad n = 0, 1, 2, \dots \quad (2.15)$$

with $\beta^{(2n+1)}$ being linear in the anomaly X given in (2.4), and the first three of them being given by

$$\beta^{(1)} = 0, \quad (2.16)$$

$$\beta^{(3)} = i\omega \partial_-^2 \varphi X,$$

$$\beta^{(5)} = i\omega \left[\frac{3}{2} \omega^2 (\partial_- \varphi)^2 \partial_-^2 \varphi + \partial_-^4 \varphi \right] X.$$

Working with the x and t variables we have that (2.15) takes the form $\partial_t a_x^{(2n+1)} - \partial_x a_t^{(2n+1)} = -\frac{1}{2} \beta^{(2n+1)}$ and so we find that

$$\frac{dQ^{(2n+1)}}{dt} = -\frac{1}{2} \alpha^{(2n+1)} + a_t^{(2n+1)} \Big|_{x=-\infty}^{x=\infty} \quad (2.17)$$

with

$$Q^{(2n+1)} \equiv \int_{-\infty}^{\infty} dx a_x^{(2n+1)}, \quad \alpha^{(2n+1)} \equiv \int_{-\infty}^{\infty} dx \beta^{(2n+1)}. \quad (2.18)$$

As we are interested in finite energy solutions of the theory (2.1) we are concerned with field configurations satisfying the boundary conditions

$$\partial_\mu \varphi \rightarrow 0; \quad V(\varphi) \rightarrow \text{global minimum} \quad \text{as} \quad x \rightarrow \pm\infty. \quad (2.19)$$

Therefore from (2.2) we see that

$$A_+ \rightarrow \frac{1}{2} (\omega^2 V_{\text{vac.}} - m) b_1, \quad A_- \rightarrow \frac{1}{2} b_{-1} \quad \text{as} \quad x \rightarrow \pm\infty, \quad (2.20)$$

where $V_{\text{vac.}}$ is the value of the potential at the global minimum which, in general, is taken to be zero. As we have seen the parameters ζ_n of the gauge (2.7) and (2.8) are polynomials in x_- -derivatives of the field φ (see appendix B). Therefore, for finite energy solutions we see that $g \rightarrow 1$ as $x \rightarrow \pm\infty$, and so

$$\begin{aligned} a_t^{(-1)} &\rightarrow \frac{1}{4}, \\ a_t^{(1)} &\rightarrow \frac{1}{4} (\omega^2 V_{\text{vac.}} - m) \quad \text{as} \quad x \rightarrow \pm\infty, \\ a_t^{(2n+1)} &\rightarrow 0 \quad n = 1, 2, \dots \end{aligned} \quad (2.21)$$

We can also investigate this behaviour more explicitly by analyzing (2.12), (2.14), (2.4) and (2.19). Consequently, for finite energy solutions satisfying (2.19), we have that

$$\frac{dQ^{(1)}}{dt} = 0, \quad \frac{dQ^{(2n+1)}}{dt} = -\frac{1}{2}\alpha^{(2n+1)} \quad n = 1, 2, \dots \quad (2.22)$$

Of course, the theory (2.1) is invariant under space-time translations and so its energy momentum tensor is conserved. The conserved charge $Q^{(1)}$ is in fact a combination of the energy and momentum of the field configuration. In section 3 we will analyze the anomalies $\alpha^{(2n+1)}$ for a concrete perturbation of the sine-Gordon model, and we will show that even though the charges are not exactly conserved they lead to very important consequences for the dynamics of the soliton solutions.

A result that we can draw for general potentials, thus, is the following. For static finite energy solutions the charges $Q^{(2n+1)}$ are obviously time independent, and as a consequence of (2.22) one sees that the anomalies vanish, *i.e.* $\alpha^{(2n+1)} = 0$. Under a $(1+1)$ -dimensional Lorentz transformation where $x_{\pm} \rightarrow \gamma^{\pm 1} x_{\pm}$ one finds that the connection (2.2) does not really transform as a vector. However, consider the internal transformation

$$A_{\mu} \rightarrow \gamma^d A_{\mu} \gamma^{-d} \quad (2.23)$$

where d is the grading operator introduced in (A.3). Then, one notices that A_{μ} , given in (2.2), transforms as a vector under the combination of the external Lorentz transformation and the internal transformation (2.23). For the same reasons the transformed connection a_{μ} , defined in (2.7), is also a vector under the combined transformations. Consequently, the anomalies $\beta^{(2n+1)}$, introduced in (2.15), are pseudo-scalars under the same combined transformation. Therefore, in any Lorentz reference frame the integrated anomalies $\alpha^{(2n+1)}$, defined in (2.18), satisfy

$$\alpha^{(2n+1)} = 0 \quad \text{for any static or a travelling finite energy solution} \quad (2.24)$$

where by a *travelling solution* we mean any solution that can be put at rest by a Lorentz boost. Even though this result may look trivial, it can perhaps shed some light on the nature of the anomalies $\alpha^{(2n+1)}$. In fact, as we will see in our concrete example of section 3, the anomalies vanish in multi-soliton solutions when the solitons they describe are far apart and so when they are not in interaction with each other. The anomalies seem to be turned on only when the interaction takes place among the solitons.

2.1 A second set of quasi conserved charges

Note that we can also construct a second set of quasi conserved charges for the theories (2.1) using another zero curvature representation of their equations of motion. The new Lax

potentials are obtained from (2.2) by interchanging x_+ with x_- , and by reverting the grades of the generators. Then we introduce the Lax potentials

$$\begin{aligned}\tilde{A}_- &= \frac{1}{2} \left[(\omega^2 V - m) b_{-1} - i \omega \frac{dV}{d\varphi} F_{-1} \right], \\ \tilde{A}_+ &= \frac{1}{2} b_1 - \frac{i}{2} \omega \partial_+ \varphi F_0.\end{aligned}\tag{2.25}$$

In this case using the commutation relations of appendix A we observe that the curvature of such a connection is

$$\tilde{F}_{+-} \equiv \partial_+ \tilde{A}_- - \partial_- \tilde{A}_+ + [\tilde{A}_+, \tilde{A}_-] = \tilde{X} F_{-1} + \frac{i}{2} \omega \left[\partial^2 \varphi + \frac{\partial V}{\partial \varphi} \right] F_0\tag{2.26}$$

with

$$\tilde{X} = -\frac{i}{2} \omega \partial_+ \varphi \left[\frac{d^2 V}{d\varphi^2} + \omega^2 V - m \right].\tag{2.27}$$

The construction of the corresponding charges follows the same procedure as in section 2. We perform the gauge transformation

$$\tilde{A}_\mu \rightarrow \tilde{a}_\mu = \tilde{g} \tilde{A}_\mu \tilde{g}^{-1} - \partial_\mu \tilde{g} \tilde{g}^{-1}\tag{2.28}$$

with the group element being

$$\tilde{g} = \exp \left[\sum_{n=1}^{\infty} \zeta_{-n} F_{-n} \right]\tag{2.29}$$

and analogously to the case of section 2, we choose the ζ_{-n} 's to cancel the F_{-n} 's components of \tilde{a}_+ . We then have

$$\partial_+ \tilde{a}_- - \partial_- \tilde{a}_+ + [\tilde{a}_+, \tilde{a}_-] = \tilde{X} \tilde{g} F_{-1} \tilde{g}^{-1}\tag{2.30}$$

where we have used the equation of motion (2.1) to cancel the component of \tilde{F}_{+-} in the direction of F_0 . The details of the calculations are given in the appendix C. The transformed connection takes the form

$$\begin{aligned}\tilde{a}_+ &= \frac{1}{2} b_1 + \sum_{n=0}^{\infty} \tilde{a}_+^{(-2n-1)} b_{-2n-1}, \\ \tilde{a}_- &= \sum_{n=0}^{\infty} \tilde{a}_-^{(-2n-1)} b_{-2n-1} + \sum_{n=2}^{\infty} \tilde{c}_+^{(-n)} F_{-n}.\end{aligned}$$

The transformed curvature (2.30) leads to equations of the form

$$\partial_+ \tilde{a}_-^{(-2n-1)} - \partial_- \tilde{a}_+^{(-2n-1)} = \tilde{\beta}^{(-2n-1)} \quad n = 0, 1, 2, \dots\tag{2.31}$$

with $\tilde{\beta}^{(2n+1)}$ being linear in the anomaly \tilde{X} , given in (2.27), and the first three are given by

$$\begin{aligned}\tilde{\beta}^{(-1)} &= 0, \\ \tilde{\beta}^{(-3)} &= i\omega \partial_+^2 \varphi \tilde{X}, \\ \tilde{\beta}^{(-5)} &= i\omega \left[\frac{3}{2} \omega^2 (\partial_+ \varphi)^2 \partial_+^2 \varphi + \partial_+^4 \varphi \right] \tilde{X}.\end{aligned}$$

Following the same reasoning as in section 2, we find that for finite energy solutions we have the quasi conservation laws

$$\frac{d\tilde{Q}^{(-1)}}{dt} = 0, \quad \frac{d\tilde{Q}^{(-2n-1)}}{dt} = -\frac{1}{2} \tilde{\alpha}^{(-2n-1)} \quad n = 1, 2, \dots \quad (2.32)$$

with

$$\tilde{Q}^{(-2n-1)} \equiv \int_{-\infty}^{\infty} dx \tilde{a}_x^{(-2n-1)}, \quad \tilde{\alpha}^{(-2n-1)} \equiv \int_{-\infty}^{\infty} dx \tilde{\beta}^{(-2n-1)}. \quad (2.33)$$

3 The expansion around the sine-Gordon model

The construction of quasi conserved charges of section 2 was performed for a very general potential, and no estimates were done on how small the anomaly of the zero curvature condition really is. We now turn to the problem of evaluating the anomalies $\alpha^{(2n+1)}$, introduced in (2.18), and to discuss the usefulness of the quasi conservation laws (2.22). In order to do that we choose a specific potential which is a perturbation of the sine-Gordon potential and that preserves its main features like infinite degenerate vacua and the existence of soliton-like solutions. So we consider the potential given in (1.1) and we put $n = 2 + \varepsilon$ *i.e.* we take

$$V(\varphi, \varepsilon) = \frac{2}{(2 + \varepsilon)^2} \tan^2 \varphi \left[1 - |\sin \varphi|^{2+\varepsilon} \right]^2. \quad (3.1)$$

In order to analyze the role of zero curvature anomalies we shall expand the equation of motion (2.1) for the potential (3.1), as well as the solutions, in powers of ε . We then write

$$\varphi = \varphi_0 + \varphi_1 \varepsilon + \varphi_2 \varepsilon^2 + \dots \quad (3.2)$$

and

$$\begin{aligned}\frac{\partial V}{\partial \varphi} &= \frac{\partial V}{\partial \varphi} \Big|_{\varepsilon=0} + \left[\frac{d}{d\varepsilon} \left(\frac{\partial V}{\partial \varphi} \right) \right]_{\varepsilon=0} \varepsilon + \dots \\ &= \frac{\partial V}{\partial \varphi} \Big|_{\varepsilon=0} + \left[\frac{\partial^2 V}{\partial \varepsilon \partial \varphi} + \frac{\partial^2 V}{\partial \varphi^2} \frac{\partial \varphi}{\partial \varepsilon} \right]_{\varepsilon=0} \varepsilon + \dots\end{aligned}$$

Using the results of appendix D, where we give the detailed calculations of such expansion, we have that the order zero field φ_0 must satisfies the sine-Gordon equation, *i.e.*

$$\partial^2 \varphi_0 + \frac{1}{4} \sin(4\varphi_0) = 0. \quad (3.3)$$

On the other hand the first order field φ_1 has to satisfy the equation

$$\partial^2 \varphi_1 + \cos(4\varphi_0) \varphi_1 = \sin(\varphi_0) \cos(\varphi_0) \left[2 \sin^2 \varphi_0 \ln(\sin^2(\varphi_0)) + \cos^2(\varphi_0) \right]. \quad (3.4)$$

We shall consider here only the anomalies for the charges constructed in section 2 (the analysis for the charges constructed in section 2.1 is very similar). We expand the anomaly X introduced in (2.4) as

$$X = X_0 + X_1 \varepsilon + X_2 \varepsilon^2 + \dots \quad (3.5)$$

and we also expand the parameters

$$\begin{aligned} \omega &= \omega_0 + \omega_1 \varepsilon + \omega_2 \varepsilon^2 + \dots \\ m &= m_0 + m_1 \varepsilon + m_2 \varepsilon^2 + \dots \end{aligned} \quad (3.6)$$

Then we find that

$$X_0 = \frac{i\omega_0}{2} \partial_- \varphi_0 \left[\frac{d^2 V}{d\varphi^2} \Big|_{\varepsilon=0} + \omega_0^2 V \Big|_{\varepsilon=0} - m_0^2 \right]. \quad (3.7)$$

Using the results of appendix D we find that X_0 vanishes by an appropriate choice of parameters, *i.e.*

$$X_0 = 0 \quad \text{when} \quad \omega_0 = 4 \quad \text{and} \quad m_0 = 1. \quad (3.8)$$

With such a choice the first order contribution to X reduces to (again using the results of appendix D)

$$\begin{aligned} X_1 &= i 2 \partial_- \varphi_0 \left[-6 \sin^2 \varphi_0 \ln(\sin^2 \varphi_0) - \cos^2 \varphi_0 - m_1^2 \right. \\ &\quad \left. + 8 \left(\frac{\omega_1}{2} - 1 \right) \sin^2 \varphi_0 \cos^2 \varphi_0 \right] \end{aligned} \quad (3.9)$$

and so we see that X_1 does not depend upon φ_1 .

Since the anomalies $\alpha^{(2n+1)}$, introduced in (2.18), are linear in X and since $X_0 = 0$, it follows that their zero order contribution vanishes, as it should since sine-Gordon is integrable. Thus we write our anomalies as

$$\alpha^{(2n+1)} = \alpha_1^{(2n+1)} \varepsilon + \alpha_2^{(2n+1)} \varepsilon^2 + \dots \quad (3.10)$$

and the first order contribution to the first two of them are (remember that $\alpha^{(1)} = 0$)

$$\begin{aligned} \alpha_1^{(3)} &= i \omega_0 \int_{-\infty}^{\infty} dx X_1 \partial_-^2 \varphi_0, \\ \alpha_1^{(5)} &= i \omega_0 \int_{-\infty}^{\infty} dx X_1 \left[\frac{3}{2} \omega_0^2 (\partial_- \varphi_0)^2 \partial_-^2 \varphi_0 + \partial_-^4 \varphi_0 \right] \end{aligned} \quad (3.11)$$

with X_1 given in (3.9). Thus, the first order anomalies do not depend on the first order field φ_1 . The first order charges, however, do depend upon φ_1 . To see this we expand the charges as

$$Q^{(2n+1)} = Q_0^{(2n+1)} + Q_1^{(2n+1)} \varepsilon + Q_2^{(2n+1)} \varepsilon^2 + \dots \quad (3.12)$$

Then we find that $Q_0^{(2n+1)}$ are conserved and correspond to the charges of the sine-Gordon model, and involve φ_0 only. As an example we present the first charge at first order

$$\begin{aligned} Q_1^{(3)} = & \int_{-\infty}^{\infty} dx \left[8 (\partial_- \varphi_0)^3 (\omega_1 \partial_- \varphi_0 + 4 \partial_- \varphi_1) + \partial_-^3 \varphi_0 (\omega_1 \partial_- \varphi_0 + 2 \partial_- \varphi_1) \right. \\ & \left. + 2 \partial_-^3 \varphi_1 \partial_- \varphi_0 + \frac{1}{4} \sin(4 \varphi_0) (\omega_1 \partial_-^2 \varphi_0 + 2 \partial_-^2 \varphi_1) - 2 \partial_-^2 \varphi_0 \partial_+ \partial_- \varphi_1 - i X_1 \partial_- \varphi_0 \right] \end{aligned}$$

which, indeed, does depend on φ_1 .

We can now evaluate the anomaly, to first order, for some physical relevant solutions of the theory (2.1) with the potential given by (3.1). As we have stressed this earlier the first order anomaly depends only upon the zero order field φ_0 which is an exact solution of the sine-Gordon equation (3.3).

3.1 Anomaly for the kink

First we look at the case of one kink. The kink solution is given by (1.2) with $n = 2 + \varepsilon$ and it is an exact solution of (2.1) for V given by (3.1). The first order anomaly depends upon the kink solution of the sine-Gordon equation (3.3) which is given by

$$\varphi_0 = \arctan(e^x). \quad (3.13)$$

Inserting this expression into (3.11) and (3.9) we find that

$$\alpha_1^{(3)} = \alpha_1^{(5)} = \int_{-\infty}^{\infty} dx \frac{\sinh x}{\cosh^4 x} \left[6 e^x \ln \left(\frac{1}{2} \frac{e^x}{\cosh x} \right) + e^{-x} \right]. \quad (3.14)$$

This expression can be integrated explicitly using the fact that

$$\frac{d}{dx} \left[\frac{2 \sinh(x) + e^x (e^{2x} - 3) \ln \left(\frac{1}{2} \frac{e^x}{\cosh x} \right)}{2 \cosh^3(x)} \right] = \frac{\sinh x}{\cosh^4 x} \left[6 e^x \ln \left(\frac{1}{2} \frac{e^x}{\cosh x} \right) + e^{-x} \right]$$

and so

$$\int_{-\infty}^{\infty} dx \frac{\sinh x}{\cosh^4 x} \left[6 e^x \ln \left(\frac{1}{2} \frac{e^x}{\cosh x} \right) + e^{-x} \right] = 0. \quad (3.15)$$

Therefore, the first order anomalies vanish, *i.e.* $\alpha_1^{(3)} = \alpha_1^{(5)} = 0$, agreeing with the general result shown in (2.24).

3.2 Anomalies for the 2-soliton solutions

3.2.1 The soliton/anti-soliton scattering

Let us consider a 2-soliton solution corresponding, for $\eta = 1$, to a soliton moving to the right with speed v and located at $x = -L$ at $t = 0$, and an anti-soliton moving to the left with speed v and located at $x = L$ at $t = 0$. For $\eta = -1$ the roles of soliton and anti-soliton are interchanged. The solution at order zero in the ε -expansion is given by a solution of the sine-Gordon equation (3.3) given by

$$\varphi_0 = \text{ArcTan} \left[\frac{\eta v \cosh y_1}{\sinh \tau_1} \right] \quad (3.16)$$

with

$$y_1 = \frac{x}{\sqrt{1-v^2}}, \quad \tau_1 = \frac{vt-L}{\sqrt{1-v^2}} + \eta \ln v. \quad (3.17)$$

Putting this expression into (3.11) and (3.9) we find that the first anomaly at first order is

$$\begin{aligned} \alpha_1^{(3)} &= \frac{8v^2}{(1-v^2)^{3/2}} \sinh \tau_1 \cosh \tau_1 \int_{-\infty}^{\infty} dx \frac{1}{\Lambda_1^3} \left[v \left((3+v^2) \Omega_1 + 4v^2 \right) \cosh^2 y_1 - 2v \Omega_1 \right] \times \\ &\times \left[-6 \frac{v^2 \cosh^2 y_1}{\Lambda_1} \ln \left(\frac{v^2 \cosh^2 y_1}{\Lambda_1} \right) - \frac{\sinh^2 \tau_1}{\Lambda_1} - m_1^2 + 8 \left(\frac{\omega_1}{2} - 1 \right) \frac{v^2 \cosh^2 y_1}{\Lambda_1} \frac{\sinh^2 \tau_1}{\Lambda_1} \right], \end{aligned} \quad (3.18)$$

where we have introduced

$$\Lambda_1 = \sinh^2 \tau_1 + v^2 \cosh^2 y_1, \quad \Omega_1 = \sinh^2 \tau_1 - v^2 \cosh^2 y_1. \quad (3.19)$$

Note that $\alpha_1^{(3)}$ given in (3.18), is an odd function of τ_1 due to the term $\sinh \tau_1$ in front of the integral. All other terms involving τ_1 in (3.18) appear as $\cosh \tau_1$ or $\sinh^2 \tau_1$, and so are even in τ_1 . Consequently we see that

$$\int_{-\infty}^{\infty} dt \alpha_1^{(3)} = 0. \quad (3.20)$$

We point out that this result is independent of the values of ω_1 and m_1 which appear in the expression for $\alpha_1^{(3)}$. Note that, from (2.22), (3.10) and (3.12), we have that

$$\frac{dQ_1^{(3)}}{dt} = -\frac{1}{2} \alpha_1^{(3)} \quad (3.21)$$

and so

$$Q_1^{(3)}(t = \infty) = Q_1^{(3)}(t = -\infty). \quad (3.22)$$

Thus, in the scattering of the soliton and anti-soliton the charge at first order is conserved asymptotically. From the physical point of view that is as effective as in the case of the integrable sine-Gordon theory. The solitons have to scatter preserving higher charges (at least in first order approximation).

3.2.2 The soliton/soliton scattering

Next we consider a 2-soliton solution corresponding, for $\eta = 1$, to a soliton moving to the right with speed v and located at $x = -L$ at $t = 0$, and another soliton moving to the left with speed v and located at $x = L$ at $t = 0$. For $\eta = -1$ the roles of soliton and anti-soliton are interchanged. The solution, at order zero in the ε -expansion, is again given by a solution of the sine-Gordon equation (3.3), namely

$$\varphi_0 = \text{ArcTan} \left[\frac{-\eta \cosh \tau_2}{v \sinh y_2} \right], \quad (3.23)$$

where

$$y_2 = \frac{x}{\sqrt{1-v^2}} + \eta \ln v, \quad \tau_2 = \frac{vt - L}{\sqrt{1-v^2}}. \quad (3.24)$$

Following the same procedure as in the case of soliton/anti-soliton solution, by putting (3.23) into (3.11) and (3.9) we find that the first anomaly, at first order, is

$$\begin{aligned} \alpha_1^{(3)} &= \frac{8v^2}{(1-v^2)^{3/2}} \sinh \tau_2 \cosh \tau_2 \int_{-\infty}^{\infty} dx \frac{1}{\Lambda_2^3} \left[v \left((v^2 + 3) \Omega_2 - 4v^2 \right) \sinh^2 y_2 + 2v \Omega_2 \right] \\ &\times \left[-6 \frac{\cosh^2 \tau_2}{\Lambda_2} \ln \left(\frac{\cosh^2 \tau_2}{\Lambda_2} \right) - \frac{v^2 \sinh^2 y_2}{\Lambda_2} - m_1^2 + 8 \left(\frac{\omega_1}{2} - 1 \right) \frac{\cosh^2 \tau_2}{\Lambda_2} \frac{v^2 \sinh^2 y_2}{\Lambda_2} \right] \end{aligned} \quad (3.25)$$

with

$$\Lambda_2 = \cosh^2 \tau_2 + v^2 \sinh^2 y_2, \quad \Omega_2 = \cosh^2 \tau_2 - v^2 \sinh^2 y_2. \quad (3.26)$$

Again, one notices that $\alpha_1^{(3)}$ given in (3.25) is odd in τ_2 . Indeed, except for the factor $\sinh \tau_2$ in front of the integral, all other terms are even in τ_2 since they involve only $\cosh \tau_2$. Consequently, we again have

$$\int_{-\infty}^{\infty} dt \alpha_1^{(3)} = 0 \quad (3.27)$$

and such result is independent of the values of ω_1 and m_1 . Again, using (3.21) we see that $Q_1^{(3)}(t = \infty) = Q_1^{(3)}(t = -\infty)$. So, the solitons scatter preserving higher charges asymptotically, like in the case of soliton/anti-soliton scattering discussed above.

3.3 Anomalies for breathers

As we show in the next section the theory (2.1) with potential (3.1) has long lived breather-like solutions. Hence, next we evaluate the anomaly, to first order, for such a solution. For that we

need the solution for the zero order field φ_0 which is a breather solution for the sine-Gordon equation (3.3), *i.e.*

$$\varphi_0 = \arctan \left(\frac{\sqrt{1-\nu^2}}{\nu} \frac{\sin(\nu t)}{\cosh(\sqrt{1-\nu^2} x)} \right), \quad (3.28)$$

where ν is the frequency of the breather ($0 < \nu < 1$), and we have chosen to express it in its Lorentz rest frame. Putting this configuration into (3.11) and (3.9) we find that the first anomaly, to first order, is

$$\alpha_1^{(3)} = -4\nu^3 (1-\nu^2) \sin(2\nu t) \left[I_1(\nu, t) - m_1^2 I_2(\nu, t) + 8 \left(\frac{\omega_1}{2} - 1 \right) I_3(\nu, t) \right] \quad (3.29)$$

with

$$\begin{aligned} I_1(\nu, t) &= \int_{-\infty}^{\infty} dx \left[2(1-\nu^2) \sinh^2(\sqrt{1-\nu^2} x) \Omega \right. \\ &+ \left. \cosh^2(\sqrt{1-\nu^2} x) \left((1-2\nu^2) \Omega - 4\nu^2 (1-\nu^2) \right) \right] \times \\ &\times \frac{1}{\Lambda^3} \left[-6 \frac{(1-\nu^2) \sin^2(\nu t)}{\Lambda} \ln \left(\frac{(1-\nu^2) \sin^2(\nu t)}{\Lambda} \right) - \frac{\nu^2 \cosh^2(\sqrt{1-\nu^2} x)}{\Lambda} \right] \end{aligned} \quad (3.30)$$

and

$$\begin{aligned} I_2(\nu, t) &= \int_{-\infty}^{\infty} dx \left[2(1-\nu^2) \sinh^2(\sqrt{1-\nu^2} x) \Omega \right. \\ &+ \left. \cosh^2(\sqrt{1-\nu^2} x) \left((1-2\nu^2) \Omega - 4\nu^2 (1-\nu^2) \right) \right] \frac{1}{\Lambda^3} \end{aligned} \quad (3.31)$$

and

$$\begin{aligned} I_3(\nu, t) &= \int_{-\infty}^{\infty} dx \left[2(1-\nu^2) \sinh^2(\sqrt{1-\nu^2} x) \Omega \right. \\ &+ \left. \cosh^2(\sqrt{1-\nu^2} x) \left((1-2\nu^2) \Omega - 4\nu^2 (1-\nu^2) \right) \right] \times \\ &\times \frac{1}{\Lambda^3} \left[\frac{\nu^2 (1-\nu^2) \sin^2(\nu t) \cosh^2(\sqrt{1-\nu^2} x)}{\Lambda^2} \right], \end{aligned} \quad (3.32)$$

where we have denoted

$$\begin{aligned} \Lambda &= \nu^2 \cosh^2(\sqrt{1-\nu^2} x) + (1-\nu^2) \sin^2(\nu t), \\ \Omega &= \nu^2 \cosh^2(\sqrt{1-\nu^2} x) - (1-\nu^2) \sin^2(\nu t). \end{aligned} \quad (3.33)$$

Note that the time dependence of the integrals $I_j(\nu, t)$, $j = 1, 2, 3$, comes only through the factor $\sin^2(\nu t) = \frac{1}{2} [1 - \cos(2\nu t)]$. Since these integrals are multiplied by the factor $\sin(2\nu t)$ in (3.29), we conclude that $\alpha_1^{(3)}$ is periodic in time with period $T \equiv \frac{\pi}{\nu}$. In addition, we observe

that $I_j(\nu, t) = I_j(\nu, -t)$, and so $\alpha_1^{(3)}(t) = -\alpha_1^{(3)}(-t)$, due to the overall factor $\sin(2\nu t)$ in (3.29). Consequently, we have that

$$\int_t^{t+T} dt' \alpha_1^{(3)}(t') = \int_{-T/2}^{T/2} dt' \alpha_1^{(3)}(t') = 0, \quad (3.34)$$

where we have used the fact that $\int_t^{t+T} = \int_t^{-T/2} + \int_{-T/2}^{T/2} + \int_{T/2}^{t+T}$, and so the first and third integrals cancel due to the fact that $\alpha_1^{(3)}(t) = \alpha_1^{(3)}(t+T)$. Consequently, we find from (3.21) that the charge (to first order) is periodic in time

$$Q_1^{(3)}(t) = Q_1^{(3)}\left(t + \frac{\pi}{\nu}\right). \quad (3.35)$$

4 Numerical support

To check our results on the anomaly we have decided to perform various simulations of the Bazeia at al model - studying two kinks, a kink-antikink, and a system involving two kinks and an antikink.

In all our numerical work the time evolution was simulated by the fourth order Runge - Kuta method. We used various lattice grids (to make sure that our results were not contaminated by any numerical artefacts, the issue here was the size of the lattice and the lattice step). We found that to have reliable results the lattice grid (given that the kinks were of size $\sim \pm 5$) had to stretch to, at least, ± 50 . Hence most of our work was performed using even larger grids and the results given in this paper were obtained in simulations in which the lattice contained 10001 equally spaced points and stretched from -75 to 75. At the edge of the grid (in practice from -71 to -75 and from +71 to +75) we absorbed the kinetic energy of the fields. During the scattering process there was some radiation sent out towards the edges of the grid and it is this radiation that our procedure absorbed (so that we would not have any reflection of the radiation from the boundaries). Thus our procedure had the effect of simulating an infinite grid in which we looked only at the fields in a finite region. Thus, due to this absorption, the total energy seen in our simulations would decrease but this decrease could be associated with the system radiating some energy towards the boundaries and the energy seen by us corresponded to the energy of the system that we have tried to describe.

4.1 Kink-kink interactions

First we looked at the interaction between 2 kinks. To study this we placed two kinks at some distance from each other and then performed a simulation to see what happens.

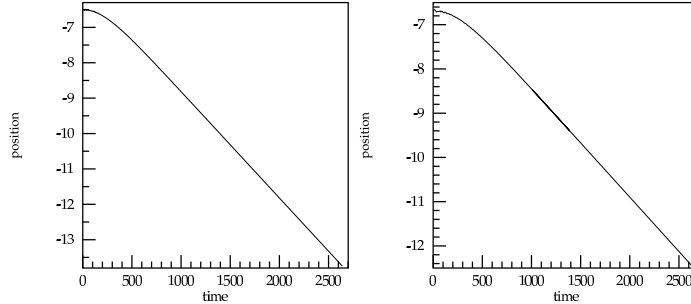


Figure 4: Trajectories: a) $n = 2$, b) $n = 1.9$,

When we performed this simulation with static kinks we have found that the kinks repel. To decide what happens during the scattering we decided to plot the positions of the kinks as a function of time. There are several possible definitions of ‘the position of the kink’ but, physically the most sensible one, involves looking at the energy density of each kink, with the position being defined at the location of the maximum of this density. This is the definition we have used in our analysis.

In fig.4 we present the trajectories of two kinks (given the definition of the position as mentioned above), initially at rest, as seen in simulations for $n = 2$ and $n = 1.9$. The kinks were initially placed at $d = \pm 7.0$ and so far away from any boundary.

It is clear from these plots that the kinks repel. We have repeated our simulations for various values of n and each time the situation was the same. Looking at the plots of the trajectories we do not see much difference between $n = 2$ and $n = 1.9$.

Next we sent the kinks towards each other with some velocities. In the fig. 5 we present the trajectories of kinks sent towards each other with velocity $v = 0.5$ for the cases corresponding to $n = 2$ and $n = 1.9$. Initially the kinks were placed at $d = \pm 15.5$

In both cases the kinks clearly come very close towards each other but then they repel and move away from each other. At larger velocities they get closer before their repulsion always sends them back. Similar results were obtained for other values of d , n and their velocities.

Incidentally, the sine-Gordon model (*i.e.* the model with $n = 2$) possesses a solution describing two moving kinks and our results (for $n = 2$) reproduce them very well and, surprise, surprise, the model does not have any static solutions involving more than one kink.

On the other hand, the sine-Gordon moving kinks solutions are known in an explicit form, and because these kinks are described by explicit functions it is often said that the “kinks pass through each other”. This is clearly wrong when one looks at the energy density of the

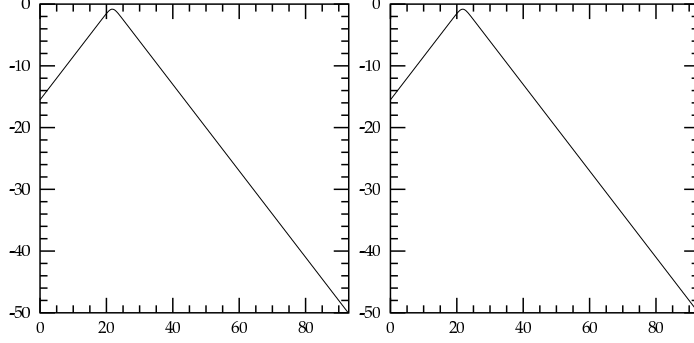


Figure 5: Trajectories: a) $n = 2$, b) $n = 1.9$,

moving kinks as they move towards each other. In fact, one easily observes that the kinks never come on top of each other (*i.e.* the two peaks of the energy density never form a double peak); in practice, the functions which describe each kink switch after the kinks' interaction.

We have also looked at the scattering of two kinks from the point of view of the integrability discussed in the previous section - *i.e.* from the point of view of the anomalies.

To do this we considered the scattering of two kinks for values of n close to 2. We looked at various positions of kinks and various velocities. All results were qualitatively similar so here we present our results for $v = .5$. The kinks were initially placed at ± 15.5 . We performed many simulations of the dynamics of such systems. In each case, as mentioned above, the kinks came close to each other, reflected and then moved to the boundaries with essentially the original velocity. Thus the scattering was very elastic. Looking at the scattering in more detail it was easy to see that, strictly speaking, there was also some radiation emitted during the scattering and that the amount of this emitted radiation increased with the increase of $|\varepsilon| = |n - 2|$; however, even for $n = 1$ this radiation constituted less than 2% of the total energy. Hence the scattering was very elastic.

We have also looked at the values of the first anomaly and its time integrated value for these scatterings.

In fig 6. we present a representative selection of our results. Fig. 6a and 6b present the time dependence of the anomaly and its time integrated form for $n = 2$, as seen in our simulations. Of course we know that for $n = 2$ the anomaly vanishes so our results provide the test of our numerics. We note that our values of the anomaly are very small - *i.e.* consistent with zero. Next we looked at the values of $n \neq 2$ for which the anomaly does not vanish. In fig 6c and 6d present our results for the anomaly and its integrated form for $n = 1.99$ and fig 6e and 6f present similar results for $n = 2.01$. Fig 6g and 6h refer to the case of $n = 1.98$

while fig 6i and 6j give the results for $n = 2.1$ and fig 6k and 6l for $n = 3$.

From these results we see very clearly that for all values of n (with the exception of $n = 3$) the integrated anomaly is approximately zero. This supports our analytical results and it shows that (for small ε) the unintegrated total anomaly is approximately proportional to $\varepsilon = n - 2$. This is supported further by the observation that the anomaly changes sign as $\varepsilon \rightarrow -\varepsilon$. The second order (in ε) effects are comparable to those of the first order and the expansion in ε clearly does not converge for $\varepsilon \sim 1$. This last point is very clear from the case of $n = 3$ in which case $\varepsilon = 1$. Of course it would be nice to understand why all the terms in the ε power series expansion are comparable in magnitude; at this stage we have no understanding of this fact.

4.2 Kink antikink scattering - quasi-breathers

Next we have looked at the kink - antikink configurations and breathers. In the sine-Gordon model we do have breathers and their analytical form is well known. They are in fact bound states of a kink and an antikink. This is all well known; what is perhaps less known, is that one can generate breathers by taking a kink and an antikink and placing them not too close to each other and then let the configuration evolve in time. As the kink and the antikink attract they move towards each other, alter their shape and, at the same time, emit some radiation and become a breather. Interestingly, they do not annihilate but do form a breather. If we then absorb the energy at the boundaries the system stabilises and essentially stops emitting further energy as the fields have taken the shape of a breather which is a time dependent solution of the model.

It is sometimes thought that the existence of breathers and of other similar configurations (wobbles etc) is, at least in part, associated with the integrability of the sine-Gordon model. Actually, as we have stressed this before, the models of Bazeia et al [1] do not appear to be integrable for any n other than 2; so we have decided to apply our procedure to look at configurations of a kink and an antikink for other values of n . However, before we discuss some of our results obtained in such cases let us first present them for the sine-Gordon model.

In fig. 7 we present the time dependence of the energy of the field configuration which involved a kink and an antikink initially placed at $d = \pm 3$ (fig 7a) and $d = \pm 5$ (fig 7b). In fig 7c we present the plot of the time dependence of the position of the kink (or antikink) for $x < 0$.

We note that in both cases (and also in other cases we have looked at, for which the results are not presented here) we have a very small initial drop of the total energy of the configuration to the energy of the resultant breather. The final energy of the breather is given

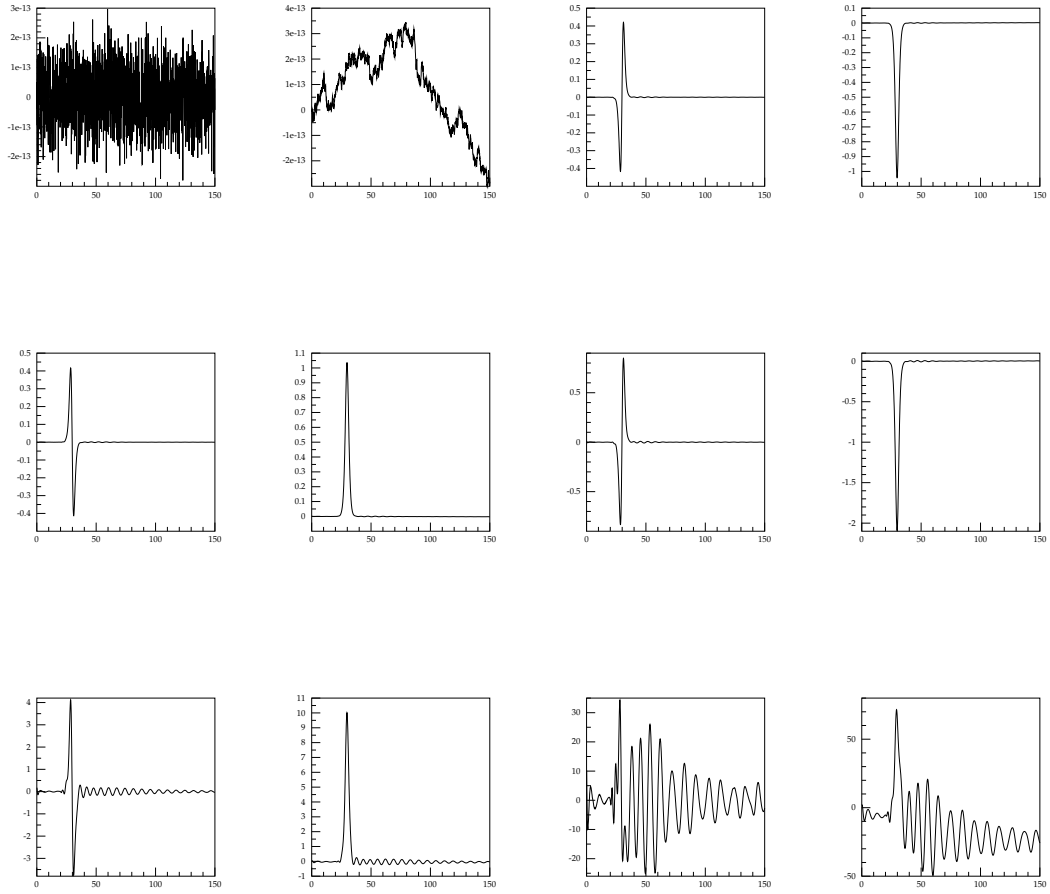


Figure 6: Anomalies and the corresponding integrated anomalies (from left to right and then down) for $n = 2.0$, $n = 1.99$, $n = 2.01$, $n = 1.98$, $n = 2.10$ and $n = 3.00$

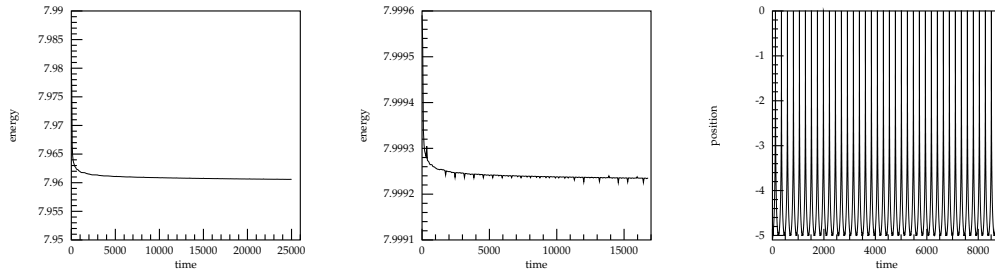


Figure 7: (ab) Time dependence of total energies; (c). Position of the kink.

by $E = 2E_0\sqrt{1 - \omega^2}$ and its frequency ω is related to the initial extend given by d .

Next, we repeated the same procedure of generating breathers for field configurations corresponding to other values of n . In fig 8. we present our results for two values of n , namely $n = 1$ and $n = 3.1$, in which the kink and the antikink were initially placed at $d = \pm 4.0$. Our plots give the time dependence of the total energy of the configuration (after the absorption at the boundaries has eliminated the radiation reaching the boundaries).

We note a fundamental difference; for $n = 1$ the energy seems to ‘stabilise’ around some finite nonzero value while for $n = 3.1$ it quickly goes to zero.

We have performed many simulations (for different values of n and for different distances between kinks and antikinks) running them for very long times. We have found that for some values of n the fields annihilate very quickly; while for the others the fields evolved towards breather-like configurations. This was not much dependent on the distance between the initial kinks but depended much more on n . In fact, as the distance d increased the whole process, like for the sine-Gordon model, was slower, the initial radiation was smaller and the generated breather was larger (and so its oscillations were slower). Looking at the dependence on n it was clear that the closer n was to 2 the more stable the breather was (this was true from about ~ 0.8 to around ~ 2.8); and for some values of n (very close to 2, like 2.01 or so) the resultant configuration was almost indistinguishable from a breather. In fact, in all such cases, the energy kept decreasing but this decrease was infinitesimal. Thus we could say that we had a **quasi-breather** (*i.e.* a long-lived breather). As the lifetime of such a quasi-breather could be counted in millions of units of time, such fields, for practical (but not purely mathematical) reasons were not very different from a breather.

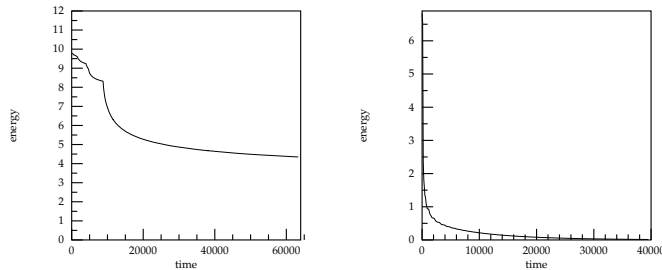


Figure 8: Time dependence of the total energy (a) $n = 1$, (b) $n = 3.1$.

In fig. 9 we present some results of our simulations (for $n = 2.01$) which demonstrate the existence of our quasi-breathers. In fig 9ab we present the plots of the field configuration for two values of t , namely $t = 355500$ and $t = 356300$. We see that the fields look very much like those of the $n = 2$ breather.

In fig. 10 ab and c we present the time dependence of the energy of the configuration on t , a detail of this dependence at large t and the time dependence of the value of field at $x = 0$. Note the extremely large values of t in the plots of the energy density. Note also the irregularity of the energy decrease. The energy gradually appears to decrease less and less and then suddenly drops and changes its slope of decrease. It then continues in the same way until the slope changes again etc. We do not understand these changes but, in any case, the total decrease of the energy is still very modest and it is clear that the quasi-breather is not going to “die” soon.

The plot in fig. 10c presents the time variation of the field at $x = 0$. As the field is symmetric around $x = 0$ this plot demonstrates the frequency of the oscillation.

We have performed similar simulations starting with the initial kinks and antikinks at other distances from each other and for other values of n . The results were qualitatively the same; the further the initial structures were - the slower was the decrease in energy (*i.e* the longer the life-time of the breather). The same was true when we considered n further away from $n = 2$. This once again suggests that the models for $n \neq 2$ (but close to 2) are quasi-integrable as discussed in the previous sections. Hence we have also looked at the behaviour of the anomaly for our quasi-breathers.

In fig. 11 ab we present the plots of the anomaly and the time integrated anomaly (at

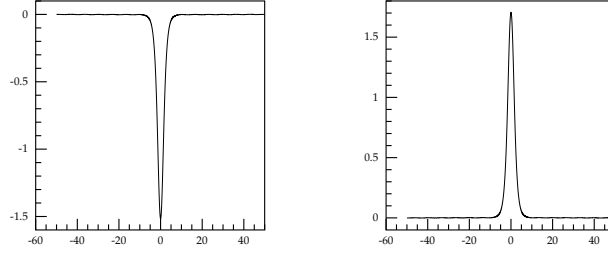


Figure 9: Field configurations (of $n = 2.01$) for (a) $t = 355500$ and (b) $t = 356300$

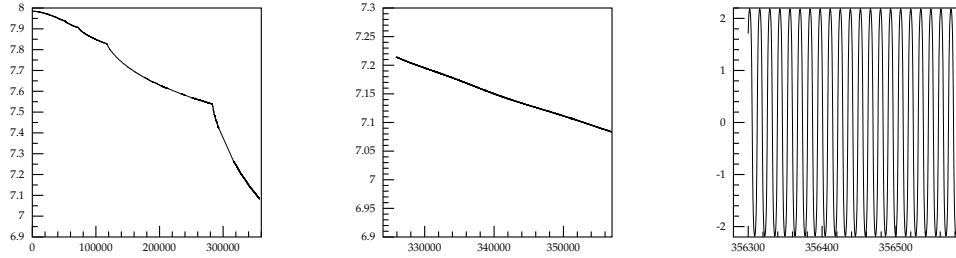


Figure 10: The time dependence of the total energy (a), of the details of this dependence at the larger values of t (b) and of the values of the field at $x = 0$ seen in a simulation of a kink and an antikink in the $n = 2.1$ model (c).

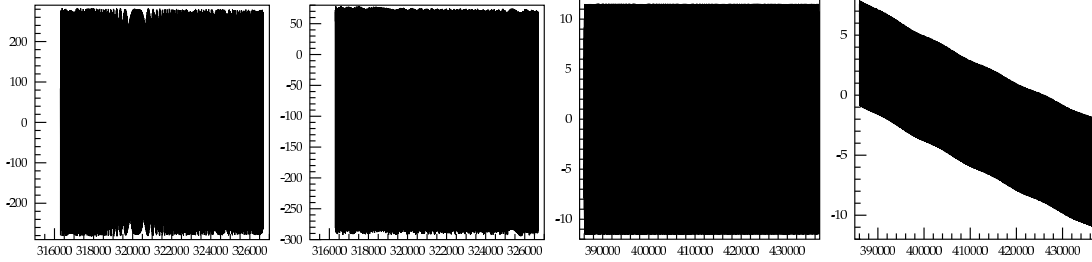


Figure 11: The first anomaly, b) the integrated first anomaly for $n = 2.01$, c) and d) the same for $n = 2.7$.

later times) of our $n = 2.01$ quasi-breather and in fig. 11 cd the similar plots for $n = 2.7$.

We see that, when compared to the two-kink case, the time integrated total anomaly is nonzero at all times (as the kink and antikink are bound into a pulsating quasi-breather) but when one looks at the time integrated anomaly over a multiple of the period of its oscillations its value is very very small (*i.e.* close to zero). For $n = 2.01$ this value is so small that it is difficult to see that it changes at all, for $n = 2.7$ the value is small but nonzero and the value changes - thus the quantity corresponding to the anomaly is, strictly speaking, not conserved.

4.3 Wobbles

Finally we looked at wobbles *i.e.*, fields involving a kink and a breather. In the sine-Gordon model they are again well known and, in fact, one has their analytical form. Of course, as before, we can generate them, numerically, from field configurations involving an antikink and two kinks (or vice-versa). However, as these configurations have an excess of energy, which is emitted when an antikink a kink form a breather, this energy can be, in part, converted into the motion of the remaining kink (or of the breather). Hence it is much harder, by comparison with pure breathers (where one can exploit the symmetry of the initial configuration), to generate non-moving wobbles. We have performed many simulations and the resultant fields sometimes were static but most of the time were moving. Clearly, the result of the simulation depends on the excess of energy - so further the initial structures were from each other the more likely there were to remain static. But this, in turn, slowed down the process of the generation of the breather. In addition, the futher n was from $n = 2$ the more radiation was sent out by the system and more likely it was that this radiation would set in motion the kink or the breather. However, for n close to 2 we did manage to obtain wobbles and in the plots given below we show some of our results.

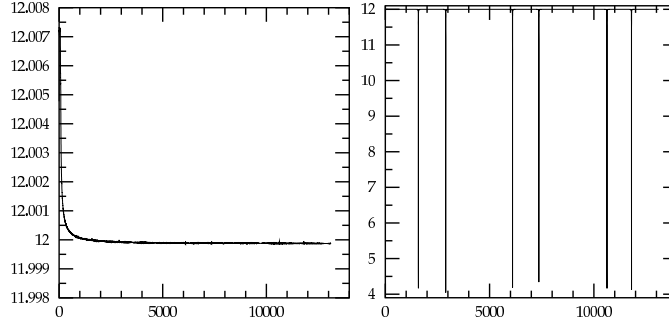


Figure 12: a) Total energy, b) Potential energy

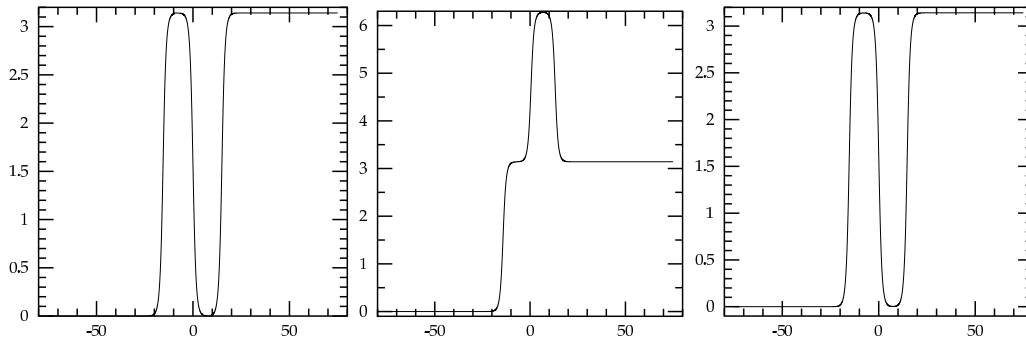


Figure 13: a) $t = 0$, b) $t = 6400$, c) $t = 12800$

First we present our results for $n = 2$, *i.e.* for the sine-Gordon model.

In fig. 12 we plot the time dependence of the total and of the potential energy seen in the simulation involving the kink, the antikink and the kink originally located at -15.5 , 0 and $+15$. In the following figure we exhibit the field configurations for three values of t , namely for $t = 0$, $t = 6400$ and $t = 12800$. We note a fast decrease of the total energy over the initial period and then stability. The potential energy is virtually always close to 12 and then it decreases to just over 4 when the breather is ‘breathing’, *i.e.* when almost all its energy is kinetic. Note that, for the breather, the flow of energy between the kinetic and the potential energies is very uneven; most of the time the breather’s energy is mainly potential and the periods over which the kinetic energy dominates are relatively short.

Next we present our results for the case of $n \neq 2$ *i.e.* $n = 2.01$. In this case the energy continues to decrease but this decrease is very slow. In fig 14c we present the details of the plot of the total energy for larger values of t . We clearly see the decrease - hence the

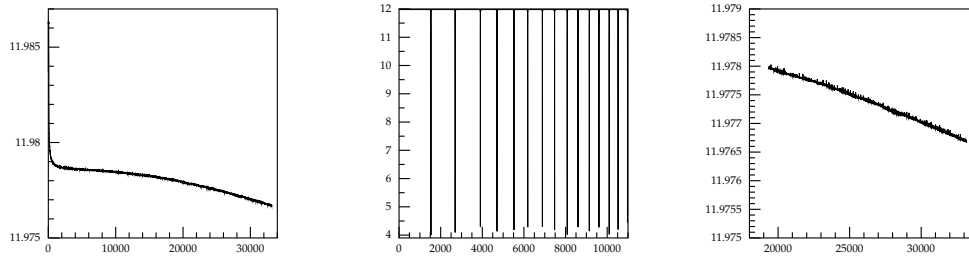


Figure 14: a) Total energy, b) Potential energy, c) Total energy for large values of t ($n = 2.01$)

breather is slowly dying but its decay is very slow indeed. And fig 15 shows the fields at some representative values of time (for $n = 2.01$). It is clearly very difficult to see any fundamental difference between the wobbles in these two systems (for $n = 2$ and $n = 2.01$), although as fig 14b shows, the time dependences of the breather oscillations in both cases are very different (much shorter for the $n = 2.01$ wobble and slowly decreasing when compared to that of $n = 2.00$).

As we have mentioned before, in our studies we have also seen simulations in which the breather and the kink which form the wobble move relative to each other. In fig 16. we show the field configurations for one of such cases. This case corresponds to $n = 1.9$.

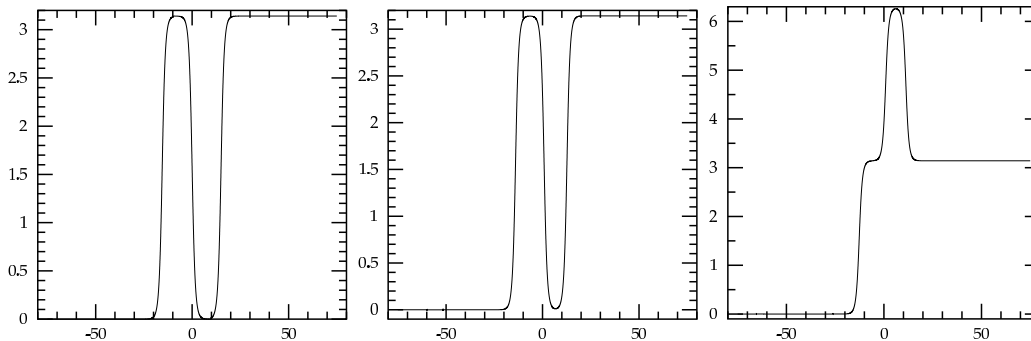


Figure 15: Fields at 3 values of t ; a) $t = 0$, b) $t = 6400$, c) $t = 12800$

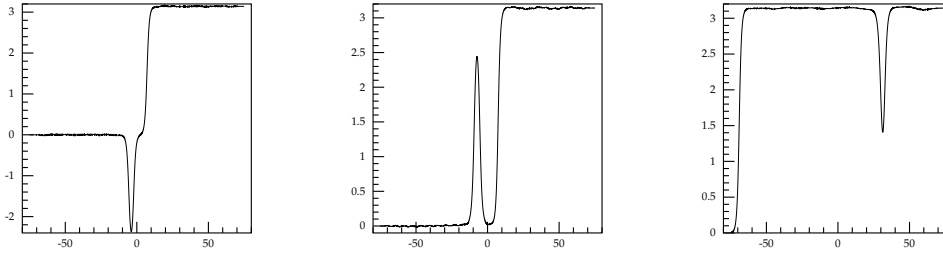


Figure 16: Fields at 3 values of t (for $n = 1.9$): a) $t = 500$, b) $t = 2000$, c) $t = 5000$.

5 Summary

In this paper we have made the first steps to introduce the concept of quasi-integrability and discussed it on the example of the models of Bazeia et al [1]. We showed that when the models are close to being integrable and so can be compared with them then one can introduce many quantities, which in the integrable case are conserved and which, in the non-integrable case, are not conserved. One can then calculate their *anomalies* that are responsible for this nonconservation, in a power series of the difference of the quasi-integrable models from their integrable neighbours. In the models of Bazeia et al [1] this difference is provided by $\varepsilon = n - 2$.

We can then calculate these anomalies for various field configurations. We have shown that the anomalies are very small for many such configurations and are only significant when the fields describe strongly time-dependent tightly bound objects; *i.e.* the field configurations like those of breathers or wobbles. And, conveniently, the models of Bazeia et al do possess such configurations.

In fact, the models of Bazeia et al, which depend on a parameter n (which when $n = 2$ reduce to the integrable sine-Gordon models) have many very similar properties and can be used to discuss the concept of quasi-integrability. All models (*i.e.* for any n) have one kink solutions and their scattering properties are very similar. Moreover, no other analytic solutions of these models (when $n \neq 2$) are known.

However, the models can be studied numerically. When we studied these models for $n \neq 2$ but close to 2 we have found that the models do, indeed, possess long-lived breather-like field

configurations; *i.e.* when we have constructed breather-like field configurations and let them evolve they gradually emitted some energy but this process was extremely slow; and so we can claim that these models (for n close to 2) possess 'very long-lived' breather-like solutions. Their life-time is closely related to how close n is to 2 and when $n < 0.8$ or $n > 2.8$ this decay was relatively fast so that the 'existence' of these states cannot be taken too seriously.

We have also looked at wobble-like states (*i.e.* states involving a breather and a kink) and the situation was found to be similar although the range of n for which such states appeared to be long lived was smaller. This is partly related to our construction of such states; we generated them all by taking initial configurations consisting of kinks and antikinks and then evolving them and absorbing, at the boundaries, any energy emitted by the configuration. For the wobble-like states, as the configuration was less symmetric the energy was emitted non-symmetrically and this often lead to more perturbation of the resultant (wobble-like) field configuration.

Thus, in addition to supporting our studies of quasi-integrability, our numerical results demonstrated also the existence of long-lived breather-like and wobble-like states.

Acknowledgements: LAF and WJZ thank the Royal Society for a grant which set up their collaboration on the topics of this paper. LAF is also partially supported by a CNPq grant while WJZ acknowledges a FAPESP grant which supported his visit to IFSC/USP.

A The algebra

We consider the $sl(2)$ algebra

$$[T_3, T_{\pm}] = \pm T_{\pm}, \quad [T_+, T_-] = 2T_3. \quad (\text{A.1})$$

We take the following basis for the corresponding loop algebra

$$b_{2m+1} = \lambda^m (T_+ + \lambda T_-), \quad F_{2m+1} = \lambda^m (T_+ - \lambda T_-), \quad F_{2m} = 2\lambda^m T_3. \quad (\text{A.2})$$

The algebra is

$$\begin{aligned} [b_{2m+1}, b_{2n+1}] &= 0, \\ [F_{2m+1}, F_{2n+1}] &= 0, \\ [F_{2m}, F_{2n}] &= 0, \\ [b_{2m+1}, F_{2n+1}] &= -2F_{2(m+n+1)}, \\ [b_{2m+1}, F_{2n}] &= -2F_{2(m+n)+1}, \\ [F_{2m+1}, F_{2n}] &= -2b_{2(m+n)+1}. \end{aligned}$$

We have a grading operator

$$d = T_3 + 2\lambda \frac{d}{d\lambda} \quad (\text{A.3})$$

such that

$$[d, b_{2m+1}] = (2m+1)b_{2m+1}, \quad [d, F_m] = mF_m. \quad (\text{A.4})$$

B The gauge transformation (2.7)

The first six parameters ζ_n of the gauge transformation (2.7), determined through (2.10) are given by

$$\begin{aligned} \zeta_1 &= \frac{1}{2}i\omega\varphi^{(0,1)}, \\ \zeta_2 &= \frac{1}{2}i\omega\varphi^{(0,2)}, \end{aligned}$$

$$\begin{aligned}
\zeta_3 &= \frac{1}{6}i \left(\omega^3(\varphi^{(0,1)})^3 + 3\omega\varphi^{(0,3)} \right), \\
\zeta_4 &= \frac{1}{6}i \left(4(\varphi^{(0,1)})^2\varphi^{(0,2)}\omega^3 + 3\varphi^{(0,4)}\omega \right), \\
\zeta_5 &= \frac{1}{30}i \left(3\omega^5(\varphi^{(0,1)})^5 + 30\omega^3\varphi^{(0,3)}(\varphi^{(0,1)})^2 + 40\omega^3(\varphi^{(0,2)})^2\varphi^{(0,1)} + 15\omega\varphi^{(0,5)} \right), \\
\zeta_6 &= \frac{1}{30}i \left(23(\varphi^{(0,1)})^4\varphi^{(0,2)}\omega^5 + 40(\varphi^{(0,2)})^3\omega^3 + 145\varphi^{(0,1)}\varphi^{(0,2)}\varphi^{(0,3)}\omega^3 \right. \\
&\quad \left. + 35(\varphi^{(0,1)})^2\varphi^{(0,4)}\omega^3 + 15\varphi^{(0,6)}\omega \right),
\end{aligned}$$

where $\varphi^{(0,n)} \equiv \partial_-^n \varphi$.

The first few components of transformed gauge potentials introduced in (2.7) are given by

$$\begin{aligned}
a_- &= \frac{1}{2}b_{-1} \\
&+ b_1 \left[-\frac{1}{4}\omega^2(\partial_- \varphi)^2 \right] \\
&+ b_3 \left[-\frac{1}{16}\omega^4(\partial_- \varphi)^4 - \frac{1}{4}\omega^2\partial_-^3 \varphi \partial_- \varphi \right] \\
&+ b_5 \left[-\frac{1}{32}\omega^6(\partial_- \varphi)^6 - \frac{7}{16}\omega^4\partial_-^3 \varphi (\partial_- \varphi)^3 - \frac{11}{16}\omega^4(\partial_-^2 \varphi)^2 (\partial_- \varphi)^2 - \frac{1}{4}\omega^2\partial_-^5 \varphi \partial_- \varphi \right] + \dots
\end{aligned}$$

and

$$\begin{aligned}
a_+ &= b_1 \left[\frac{1}{2} (\omega^2 V - m) \right] \\
&+ b_3 \left[\frac{1}{4}\omega^2 \partial_-^2 \varphi \frac{dV}{d\varphi} - \frac{1}{2}i\omega \partial_- \varphi X \right] \\
&+ b_5 \left[-\frac{3}{8}i\omega^3 (\partial_- \varphi)^3 X + \frac{5}{16}\omega^4 \partial_-^2 \varphi (\partial_- \varphi)^2 \frac{dV}{d\varphi} - \frac{1}{2}i\omega \partial_- \varphi \partial_-^2 X + \frac{1}{2}i\omega \partial_-^2 \varphi \partial_- X \right. \\
&\quad \left. - \frac{1}{2}i\omega \partial_-^3 \varphi X + \frac{1}{4}\omega^2 \partial_-^4 \varphi \frac{dV}{d\varphi} \right] \\
&+ F_2 X \\
&+ F_3 \partial_- X \\
&+ F_4 \left[\frac{1}{2}\omega^2 (\partial_- \varphi)^2 X + \partial_-^2 X \right] \\
&+ F_5 \left[\omega^2 (\partial_- \varphi)^2 \partial_- X + \frac{1}{2}\omega^2 \partial_- \varphi \partial_-^2 \varphi X + \partial_-^3 X \right] \\
&+ F_6 \left[\frac{3}{8}\omega^4 (\partial_- \varphi)^4 X + \frac{3}{2}\omega^2 (\partial_- \varphi)^2 \partial_-^2 X + \frac{5}{2}\omega^2 \partial_-^2 \varphi \partial_- \varphi \partial_- X + \omega^2 \partial_-^3 \varphi \partial_- \varphi X + \partial_-^4 X \right] + \dots
\end{aligned}$$

The anomalous terms of the gauge transformation (2.7), *i.e.*, those that do not vanish due to the anomaly X introduced in (2.4), are given by

$$\begin{aligned}
X g F_1 g^{-1} &= [a_+, a_-] = \\
& b_3 [i\omega \partial_-^2 \varphi X] \\
& + b_5 \left[\frac{3}{2} i\omega^3 (\partial_- \varphi)^2 \partial_-^2 \varphi X + i\omega \partial_-^4 \varphi X \right] \\
& + F_2 [-\partial_- X] \\
& + F_3 [-\partial_-^2 X] \\
& + F_4 \left[-\frac{1}{2} \omega^2 (\partial_- \varphi)^2 \partial_- X - \omega^2 \partial_- \varphi \partial_-^2 \varphi X - \partial_-^3 X \right] \\
& + F_5 \left[-\frac{5}{2} \omega^2 \partial_- \varphi \partial_-^2 \varphi \partial_- X - \omega^2 (\partial_- \varphi)^2 \partial_-^2 X - \frac{1}{2} \omega^2 (\partial_-^2 \varphi)^2 X - \frac{1}{2} \omega^2 \partial_- \varphi \partial_-^3 \varphi X - \partial_-^4 X \right] \\
& + \dots
\end{aligned}$$

C The gauge transformation (2.28)

The first six parameters ζ_{-n} of the gauge transformation (2.28) and (2.29) are given by

$$\begin{aligned}
\zeta_{-1} &= \frac{1}{2} i\omega \varphi^{(1,0)}, \\
\zeta_{-2} &= \frac{1}{2} i\omega \varphi^{(2,0)}, \\
\zeta_{-3} &= \frac{1}{6} i \left(\omega^3 (\varphi^{(1,0)})^3 + 3\omega \varphi^{(3,0)} \right), \\
\zeta_{-4} &= \frac{1}{6} i \left(4(\varphi^{(1,0)})^2 \varphi^{(2,0)} \omega^3 + 3\varphi^{(4,0)} \omega \right), \\
\zeta_{-5} &= \frac{1}{30} i \left(3\omega^5 (\varphi^{(1,0)})^5 + 30\omega^3 \varphi^{(3,0)} (\varphi^{(1,0)})^2 + 40\omega^3 (\varphi^{(2,0)})^2 \varphi^{(1,0)} + 15\omega \varphi^{(5,0)} \right), \\
\zeta_{-6} &= \frac{1}{30} i \left(23(\varphi^{(1,0)})^4 \varphi^{(2,0)} \omega^5 + 40(\varphi^{(2,0)})^3 \omega^3 + 145\varphi^{(1,0)} \varphi^{(2,0)} \varphi^{(3,0)} \omega^3 \right. \\
& \quad \left. + 35(\varphi^{(1,0)})^2 \varphi^{(4,0)} \omega^3 + 15\varphi^{(6,0)} \omega \right),
\end{aligned}$$

where $\varphi^{(n,0)} \equiv \partial_+^n \varphi$.

The first few components of transformed gauge potentials introduced in (2.28) are given by

$$\tilde{a}_+ = \frac{1}{2} b_1$$

$$\begin{aligned}
& + b_{-1} \left[-\frac{1}{4} \omega^2 (\partial_+ \varphi)^2 \right] \\
& + b_{-3} \left[-\frac{1}{16} \omega^4 (\partial_+ \varphi)^4 - \frac{1}{4} \omega^2 \partial_+^3 \varphi \partial_+ \varphi \right] \\
& + b_{-5} \left[-\frac{1}{32} \omega^6 (\partial_+ \varphi)^6 - \frac{7}{16} \omega^4 \partial_+^3 \varphi (\partial_+ \varphi)^3 - \frac{11}{16} \omega^4 (\partial_+^2 \varphi)^2 (\partial_+ \varphi)^2 - \frac{1}{4} \omega^2 \partial_+^5 \varphi \partial_+ \varphi \right] + \dots
\end{aligned}$$

and

$$\begin{aligned}
\tilde{a}_- & = b_{-1} \left[\frac{1}{2} (\omega^2 V - m) \right] \\
& + b_{-3} \left[\frac{1}{4} \omega^2 \partial_+^2 \varphi \frac{dV}{d\varphi} + \frac{1}{2} i \omega \partial_+ \varphi \tilde{X} \right] \\
& + b_{-5} \left[\frac{5}{16} \omega^4 \partial_+^2 \varphi (\partial_+ \varphi)^2 \frac{dV}{d\varphi} + \frac{1}{4} \omega^2 \partial_+^4 \varphi \frac{dV}{d\varphi} + \frac{3}{8} i \omega^3 (\partial_+ \varphi)^3 \tilde{X} + \frac{1}{2} i \omega \partial_+ \varphi \partial_+^2 \tilde{X} \right. \\
& \quad \left. - \frac{1}{2} i \omega \partial_+^2 \varphi \partial_+ \tilde{X} + \frac{1}{2} i \omega \partial_+^3 \varphi \tilde{X} \right] \\
& + F_{-2} \left[-\tilde{X} \right] \\
& + F_{-3} \left[-\partial_+ \tilde{X} \right] \\
& + F_{-4} \left[-\frac{1}{2} \omega^2 (\partial_+ \varphi)^2 \tilde{X} - \partial_+^2 \tilde{X} \right] \\
& + F_{-5} \left[\omega^2 (-(\partial_+ \varphi)^2) \partial_+ \tilde{X} - \frac{1}{2} \omega^2 \partial_+ \varphi \partial_+^2 \varphi \tilde{X} - \partial_+^3 \tilde{X} \right] \\
& + F_{-6} \left[-\frac{3}{8} \omega^4 (\partial_+ \varphi)^4 \tilde{X} - \frac{3}{2} \omega^2 (\partial_+ \varphi)^2 \partial_+^2 \tilde{X} - \frac{5}{2} \omega^2 \partial_+^2 \varphi \partial_+ \varphi \partial_+ \tilde{X} - \omega^2 \partial_+^3 \varphi \partial_+ \varphi \tilde{X} - \partial_+^4 \tilde{X} \right] \\
& + \dots
\end{aligned}$$

The anomalous terms of the gauge transformation (2.28), *i.e.*, those that do not vanish due to the anomaly \tilde{X} introduced in (2.27), are given by

$$\begin{aligned}
& \tilde{X} \tilde{g} F_{-1} \tilde{g}^{-1} - [\tilde{a}_+, \tilde{a}_-] = \\
& b_{-3} \left[i \omega \partial_+^2 \varphi \tilde{X} \right] \\
& + b_{-5} \left[\frac{3}{2} i \omega^3 (\partial_+ \varphi)^2 \partial_+^2 \varphi \tilde{X} + i \omega \partial_+^4 \varphi \tilde{X} \right] \\
& + F_{-2} \left[-\partial_+ \tilde{X} \right] \\
& + F_{-3} \left[-\partial_+^2 \tilde{X} \right] \\
& + F_{-4} \left[-\frac{1}{2} \omega^2 (\partial_+ \varphi)^2 \partial_+ \tilde{X} - \omega^2 \partial_+ \varphi \partial_+^2 \varphi \tilde{X} - \partial_+^3 \tilde{X} \right]
\end{aligned}$$

$$\begin{aligned}
& + F_{-5} \left[-\frac{5}{2} \omega^2 \partial_+ \varphi \partial_+^2 \varphi \partial_+ \tilde{X} - \omega^2 (\partial_+ \varphi)^2 \partial_+^2 \tilde{X} - \frac{1}{2} \omega^2 (\partial_+^2 \varphi)^2 \tilde{X} - \frac{1}{2} \omega^2 \partial_+ \varphi \partial_+^3 \varphi \tilde{X} - \partial_+^4 \tilde{X} \right] \\
& + \dots
\end{aligned}$$

D The ε -expansion

$$\begin{aligned}
V & = V|_{\varepsilon=0} + \frac{dV}{d\varepsilon} \Big|_{\varepsilon=0} \varepsilon + \dots \\
& = V|_{\varepsilon=0} + \left[\frac{\partial V}{\partial \varepsilon} + \frac{\partial V}{\partial \varphi} \frac{\partial \varphi}{\partial \varepsilon} \right]_{\varepsilon=0} \varepsilon \\
& + \left[\frac{\partial^2 V}{\partial \varepsilon^2} + 2 \frac{\partial^2 V}{\partial \varepsilon \partial \varphi} \frac{\partial \varphi}{\partial \varepsilon} + \frac{\partial V}{\partial \varphi} \frac{\partial^2 \varphi}{\partial \varepsilon^2} + \frac{\partial^2 V}{\partial \varphi^2} \left(\frac{\partial \varphi}{\partial \varepsilon} \right)^2 \right]_{\varepsilon=0} \varepsilon^2 + \dots \quad (\text{D.1})
\end{aligned}$$

Analogously, we have

$$\begin{aligned}
\frac{\partial V}{\partial \varphi} & = \frac{\partial V}{\partial \varphi} \Big|_{\varepsilon=0} + \left[\frac{d}{d\varepsilon} \left(\frac{\partial V}{\partial \varphi} \right) \right]_{\varepsilon=0} \varepsilon + \dots \\
& = \frac{\partial V}{\partial \varphi} \Big|_{\varepsilon=0} + \left[\frac{\partial^2 V}{\partial \varepsilon \partial \varphi} + \frac{\partial^2 V}{\partial \varphi^2} \frac{\partial \varphi}{\partial \varepsilon} \right]_{\varepsilon=0} \varepsilon \\
& + \left[\frac{\partial^3 V}{\partial \varepsilon^2 \partial \varphi} + 2 \frac{\partial^3 V}{\partial \varepsilon \partial \varphi^2} \frac{\partial \varphi}{\partial \varepsilon} + \frac{\partial^2 V}{\partial \varphi^2} \frac{\partial^2 \varphi}{\partial \varepsilon^2} + \frac{\partial^3 V}{\partial \varphi^3} \left(\frac{\partial \varphi}{\partial \varepsilon} \right)^2 \right]_{\varepsilon=0} \varepsilon^2 + \dots \quad (\text{D.2})
\end{aligned}$$

and

$$\begin{aligned}
\frac{\partial^2 V}{\partial \varphi^2} & = \frac{\partial^2 V}{\partial \varphi^2} \Big|_{\varepsilon=0} + \left[\frac{d}{d\varepsilon} \left(\frac{\partial^2 V}{\partial \varphi^2} \right) \right]_{\varepsilon=0} \varepsilon + \dots \\
& = \frac{\partial^2 V}{\partial \varphi^2} \Big|_{\varepsilon=0} + \left[\frac{\partial^3 V}{\partial \varepsilon \partial \varphi^2} + \frac{\partial^3 V}{\partial \varphi^3} \frac{\partial \varphi}{\partial \varepsilon} \right]_{\varepsilon=0} \varepsilon \\
& + \left[\frac{\partial^4 V}{\partial \varepsilon^2 \partial \varphi^2} + 2 \frac{\partial^4 V}{\partial \varepsilon \partial \varphi^3} \frac{\partial \varphi}{\partial \varepsilon} + \frac{\partial^3 V}{\partial \varphi^3} \frac{\partial^2 \varphi}{\partial \varepsilon^2} + \frac{\partial^4 V}{\partial \varphi^4} \left(\frac{\partial \varphi}{\partial \varepsilon} \right)^2 \right]_{\varepsilon=0} \varepsilon^2 + \dots \quad (\text{D.3})
\end{aligned}$$

Calculating we have

$$\begin{aligned}
V|_{\varepsilon=0} & = \frac{1}{8} \sin^2(2\varphi_0) = \frac{1}{16} [1 - \cos(4\varphi_0)] \\
\frac{\partial V}{\partial \varphi} \Big|_{\varepsilon=0} & = \frac{1}{4} \sin(4\varphi_0) \\
\frac{\partial^2 V}{\partial \varphi^2} \Big|_{\varepsilon=0} & = \cos(4\varphi_0)
\end{aligned}$$

$$\begin{aligned}
\frac{\partial^3 V}{\partial \varphi^3} \Big|_{\varepsilon=0} &= -4 \sin(4\varphi_0) \\
\frac{\partial^4 V}{\partial \varphi^4} \Big|_{\varepsilon=0} &= -16 \cos(4\varphi_0)
\end{aligned} \tag{D.4}$$

and

$$\begin{aligned}
\frac{\partial V}{\partial \varepsilon} \Big|_{\varepsilon=0} &= -\frac{1}{2} \sin^2(\varphi_0) \left[2 \sin^2(\varphi_0) \log |\sin(\varphi_0)| + \cos^2(\varphi_0) \right] \\
\frac{\partial^2 V}{\partial \varphi \partial \varepsilon} \Big|_{\varepsilon=0} &= -\frac{1}{4} \sin(2\varphi_0) \left[8 \sin^2 \varphi_0 \log |\sin(\varphi_0)| + \cos(2\varphi_0) + 1 \right] \\
\frac{\partial^3 V}{\partial \varphi^2 \partial \varepsilon} \Big|_{\varepsilon=0} &= -\frac{1}{2} \left[4 (\cos(2\varphi_0) - \cos(4\varphi_0)) \log |\sin(\varphi_0)| + \cos(2\varphi_0) + 1 \right] \\
\frac{\partial^4 V}{\partial \varphi^3 \partial \varepsilon} \Big|_{\varepsilon=0} &= \sin(2\varphi_0) \left[-(-4 \log |\sin(\varphi_0)| + 4 \cos(2\varphi_0)(4 \log |\sin(\varphi_0)| + 1) + 1) \right]
\end{aligned} \tag{D.5}$$

and

$$\begin{aligned}
\frac{\partial^2 V}{\partial \varepsilon^2} \Big|_{\varepsilon=0} &= \frac{1}{4} \tan^2(\varphi_0) \left[\sin^4(\varphi_0) \left(8 \log^2 |\sin(\varphi_0)| - 8 \log |\sin(\varphi_0)| + 3 \right) \right. \\
&\quad \left. + \sin^2(\varphi_0) \left(-4 \log^2 |\sin(\varphi_0)| + 8 \log |\sin \varphi_0| - 6 \right) + 3 \right] \\
\frac{\partial^3 V}{\partial \varphi \partial \varepsilon^2} \Big|_{\varepsilon=0} &= \frac{1}{32} \tan(\varphi_0) \sec^2(\varphi_0) \left[24 \log^2 |\sin(\varphi_0)| + 16 \log |\sin(\varphi_0)| \right. \\
&\quad \left. + 8 \cos(6\varphi_0) \log^2 |\sin(\varphi_0)| \right. \\
&\quad \left. + \cos(2\varphi_0) \left(-40 \log^2 |\sin(\varphi_0)| + 4 \log |\sin(\varphi_0)| + 23 \right) \right. \\
&\quad \left. + 8 \cos(4\varphi_0) (\log |\sin(\varphi_0)| - 1)^2 - 4 \cos(6\varphi_0) \log |\sin(\varphi_0)| + \cos(6\varphi_0) + 16 \right] \\
\frac{\partial^4 V}{\partial \varphi^2 \partial \varepsilon^2} \Big|_{\varepsilon=0} &= \frac{1}{16} \sec^4(\varphi_0) \left[44 \log^2 |\sin(\varphi_0)| + 16 \log |\sin(\varphi_0)| \right. \\
&\quad \left. + 10 \cos(6\varphi_0) \log^2 |\sin(\varphi_0)| + 4 \cos(8\varphi_0) \log^2 |\sin(\varphi_0)| \right. \\
&\quad \left. + 2 \cos(2\varphi_0) \left(-29 \log^2 |\sin(\varphi_0)| + \log |\sin(\varphi_0)| + 6 \right) \right. \\
&\quad \left. - 2 \cos(6\varphi_0) \log |\sin(\varphi_0)| + \cos(4\varphi_0) (3 - 16 \log |\sin(\varphi_0)|) + 9 \right]
\end{aligned} \tag{D.6}$$

References

- [1] D. Bazeia et al, arXiv:0708.1740 *Physica D* **237** (2008) 937
- [2] S. R. Coleman, “Quantum sine-Gordon equation as the massive Thirring model,” *Phys. Rev. D* **11**, 2088 (1975).
S. Mandelstam, “Soliton operators for the quantized sine-Gordon equation,” *Phys. Rev. D* **11**, 3026 (1975).
- [3] C. Montonen and D. I. Olive, “Magnetic Monopoles As Gauge Particles?,” *Phys. Lett. B* **72**, 117 (1977).
C. Vafa and E. Witten, “A Strong coupling test of S duality,” *Nucl. Phys. B* **431**, 3 (1994) [arXiv:hep-th/9408074].
N. Seiberg and E. Witten, “Electric - magnetic duality, monopole condensation, and confinement in N=2 supersymmetric Yang-Mills theory,” *Nucl. Phys. B* **426**, 19 (1994) [Erratum-ibid. *B* **430**, 485 (1994)] [arXiv:hep-th/9407087].
- [4] P. D. Lax, “Integrals Of Nonlinear Equations Of Evolution And Solitary Waves,” *Commun. Pure Appl. Math.* **21**, 467-490 (1968).
V.E. Zakharov and A.B. Shabat, *Zh. Exp. Teor. Fiz.* **61** (1971) 118-134; english transl. *Soviet Phys. JETP* **34** (1972) 62-69.
- [5] L. D. Faddeev, “Integrable models in (1+1)-dimensional quantum field theory,”; Proc. of Summer School of Theoretical Physics, Les Houches, France, Aug 2 - Sep 10, 1982. Published in *Les Houches Sum.School 1982:561 (QC175:G7:1982)*
- [6] O. Babelon, D. Bernard and M. Talon; “Introduction to Classical Integrable Systems”; Cambridge Monographs on Mathematical Physics, Cambridge University Press (2003)
- [7] W.J. Zakrzewski, *Low Dimensional Sigma Models* (Hilger, Bristol, 1989).
- [8] N. S. Manton and P. Sutcliffe, “Topological solitons,” *Cambridge, UK: Univ. Pr. (2004)* 493 p
- [9] A. B. Zamolodchikov, “Tetrahedron Equations And The Relativistic S Matrix Of Straight Strings In (2+1)-Dimensions,” *Commun. Math. Phys.* **79**, 489 (1981).
A.B. Zamolodchikov, *Zh. Eksp. Teor. Fiz.* 79, 641-664 (1980); *J.E.T.P.* 52, 325-336 (1980)
- [10] O. Alvarez, L.A. Ferreira, J. Sanchez Guillen, “A new approach to integrable theories in any dimension”, *Nucl. Phys.* **B529** (1998) 689-736, [arXiv:hep-th/9710147]
O. Alvarez, L. A. Ferreira and J. Sanchez-Guillen, “Integrable theories and loop spaces:

- fundamentals, applications and new developments,” *Int. J. Mod. Phys. A* **24**, 1825 (2009) [arXiv:0901.1654 [hep-th]].
- [11] L.A. Ferreira and W.J. Zakrzewski - ‘Some comments on quasi-integrability’ - preprint, to appear in the Proceedings of 42 Symposium on Mathematical Physics, Torun 2010, to be published in Reports on Mathematical Physics.
- [12] L. A. Ferreira, B. Piette and W. J. Zakrzewski, “Wobbles and other kink-breather solutions of the sine-Gordon model,” *Phys. Rev. E* **77**, 036613 (2008) [arXiv:0708.1088 [hep-th]].
- [13] L. A. Ferreira and W. J. Zakrzewski, “A simple formula for the conserved charges of soliton theories,” *JHEP* **0709**, 015 (2007) [arXiv:0707.1603 [hep-th]].
- [14] D. I. Olive and N. Turok, “Local Conserved Densities And Zero Curvature Conditions For Toda Lattice Field Theories,” *Nucl. Phys. B* **257**, 277 (1985).
- [15] D. I. Olive and N. Turok, “The Toda Lattice Field Theory Hierarchies And Zero Curvature Conditions In Kac-Moody Algebras,” *Nucl. Phys. B* **265**, 469 (1986).
- [16] H. Aratyn, L. A. Ferreira, J. F. Gomes and A. H. Zimerman, “The Conserved charges and integrability of the conformal affine Toda models,” *Mod. Phys. Lett. A* **9**, 2783 (1994) [arXiv:hep-th/9308086].